Journal of Hydrology 533 (2016) 250–265

Contents lists available at ScienceDirect

Journal of Hydrology

journal homepage: www.elsevier.com/locate/jhydrol

Feasibility analysis of using inverse modeling for estimating natural groundwater recharge from a large-scale soil moisture monitoring network

Tiejun Wang [a,*], Trenton E. Franz [a], Weifeng Yue [a,b], Jozsef Szilagyi [a,c], Vitaly A. Zlotnik [d], Jinsheng You [a], Xunhong Chen [a], Martha D. Shulski [a], Aaron Young [a]

[a] School of Natural Resources, University of Nebraska-Lincoln, Hardin Hall, 3310 Holdrege Street, Lincoln, NE 68583, USA
[b] College of Water Sciences, Beijing Normal University, Beijing 100875, China
[c] Department of Hydraulic and Water Resources Engineering, Budapest University of Technology and Economics, Budapest, Hungary
[d] Department of Earth and Atmospheric Sciences, University of Nebraska-Lincoln, 214 Bessey Hall, Lincoln, NE 68588, USA

ARTICLE INFO

Article history:
Received 30 September 2015
Received in revised form 7 December 2015
Accepted 10 December 2015
Available online 18 December 2015
This manuscript was handled by Corrado Corradini, Editor-in-Chief, with the assistance of Renato Morbidelli, Associate Editor

Keywords:
Groundwater recharge
Inverse modeling
Vadose zone model
Soil moisture
Automated Weather Data Network

SUMMARY

Despite the importance of groundwater recharge (*GR*), its accurate estimation still remains one of the most challenging tasks in the field of hydrology. In this study, with the help of inverse modeling, long-term (6 years) soil moisture data at 34 sites from the Automated Weather Data Network (AWDN) were used to estimate the spatial distribution of *GR* across Nebraska, USA, where significant spatial variability exists in soil properties and precipitation (*P*). To ensure the generality of this study and its potential broad applications, data from public domains and literature were used to parameterize the standard Hydrus-1D model. Although observed soil moisture differed significantly across the AWDN sites mainly due to the variations in *P* and soil properties, the simulations were able to capture the dynamics of observed soil moisture under different climatic and soil conditions. The inferred mean annual *GR* from the calibrated models varied over three orders of magnitude across the study area. To assess the uncertainties of the approach, estimates of *GR* and actual evapotranspiration (ET_a) from the calibrated models were compared to the *GR* and ET_a obtained from other techniques in the study area (e.g., remote sensing, tracers, and regional water balance). Comparison clearly demonstrated the feasibility of inverse modeling and large-scale (>10^4 km^2) soil moisture monitoring networks for estimating *GR*. In addition, the model results were used to further examine the impacts of climate and soil on *GR*. The data showed that both *P* and soil properties had significant impacts on *GR* in the study area with coarser soils generating higher *GR*; however, different relationships between *GR* and *P* emerged at the AWDN sites, defined by local climatic and soil conditions. In general, positive correlations existed between annual *GR* and *P* for the sites with coarser-textured soils or under wetter climatic conditions. With the rapidly expanding soil moisture monitoring networks around the globe, this study may have important applications in aiding water resources management in different regions.

1. Introduction

Knowledge of groundwater recharge (*GR*) is pivotal for numerous reasons, such as sustainable management of water resources and mitigation of groundwater contamination (Böhlke, 2002; Scanlon et al., 2006; Gleeson et al., 2012). However, owing to the highly nonlinear nature of the process, *GR* may vary significantly over space and time (Small, 2005; Scanlon et al., 2006). As such, accurate estimation of *GR* still remains one of the most challenging tasks in the field of hydrology (De Vries and Simmers, 2002; National Research Council, 2004). Over the past several decades, a range of techniques have been developed to quantify *GR* with various degrees of success (c.f., Allison et al., 1994; Scanlon et al., 2002). Although previous studies indicated that tracer approaches might provide the most reliable *GR* estimates (Allison et al., 1994; De Vries and Simmers, 2002), the use of process-based vadose zone models (VZMs) has recently attracted more attention, largely due to the time and cost effectiveness of this method for quantifying *GR* (Small, 2005; Jiménez-Martínez et al., 2009; Carrera-Hernández et al., 2012; Min et al., 2015; Ries et al., 2015; Turkeltaub et al., 2015).

* Corresponding author.
E-mail address: twang3@unl.edu (T. Wang).

http://dx.doi.org/10.1016/j.jhydrol.2015.12.019
0022-1694/

Compared to other methods, the use of VZMs demands complicated model parameterizations, particularly the soil hydraulic parameters (SHPs) inputs that are generally unavailable. To resolve this issue, pedotransfer functions (PTFs), which convert readily available or easily measurable soil properties (e.g., soil texture, particle size distribution, and bulk density) to SHPs (Schaap et al., 2001; Wösten et al., 2001), have been routinely used along with VZMs for quantifying *GR* at regional scales (e.g., Keese et al., 2005; Nolan et al., 2007). In spite of the advantages, the reliability of such a method for computing *GR* is greatly constrained by the uncertainties associated with PTFs, particularly in semiarid regions (Faust et al., 2006; Wang et al., 2009a, 2015a). Therefore, it is necessary to seek new approaches to estimating SHPs for computing *GR*, and inverse modeling to infer SHPs from observed soil moisture and/or matric potential data is such an approach (see the reviews by Hopmans and Simunek (1999) and Vrugt et al. (2008)). Recently, studies tested the practical viability of inverse vadose zone modeling for estimating *GR* under different soil, vegetation, and hydroclimatic conditions (Jiménez-Martínez et al., 2009; Lu et al., 2011; Andreasen et al., 2013; Min et al., 2015; Ries et al., 2015; Turkeltaub et al., 2015). By calibrating a VZM to soil moisture data in an agricultural field, Jiménez-Martínez et al. (2009) concluded that the approach of inverse modeling was promising for providing reliable *GR* estimates in semiarid regions. Andreasen et al. (2013) calibrated a 1-D soil–plant–atmosphere model using soil moisture data within a small watershed, and also reached the conclusion that inverse modeling could offer reliable *GR* estimates. Min et al. (2015) showed that *GR* estimated from inverse modeling was comparable to the one obtained from the chloride mass balance method.

Despite previous efforts, earlier inverse modeling studies mostly focused on quantifying local-scale *GR* (e.g., at one location); however, *GR* may spatially vary depending on local soil, vegetation, and hydroclimatic conditions (Keese et al., 2005; Small, 2005; Wang et al., 2015a). Thus, from the perspective of water resources management, it is more valuable to provide spatial information on *GR* at much larger spatial scales. With rapid developments in sensor technology for measuring soil moisture, soil moisture data have become increasingly accessible from large-scale distributed monitoring networks (>10^4 km^2; see Crow et al. (2012) and Ochsner et al. (2013) for the lists of large-scale soil moisture monitoring networks around the globe). Although those soil moisture monitoring networks were originally deployed for other purposes (e.g., monitoring droughts and validating remotely sensed data), they may provide additional societal benefits of estimating spatial distributions of *GR* at low costs (e.g., without additional field work and installing new equipment); however, its feasibility warrants further investigation, which is the primary motivation of this work.

The primary goal of this study was threefold: (1) use a widely-spread soil moisture monitoring network and an inverse modeling technique to estimate the spatial distribution of *GR* in a semiarid region, (2) compare the inverse modeling technique with other methods for quantifying *GR*, and (3) assess soil and climatic controls on *GR*. To ensure the generality of this study, a standard procedure was proposed to parameterize a widely used VZM. This procedure utilized publicly available data and literature values. For calibrating the VZM, long-term daily soil moisture data (i.e., 6 years) were retrieved from the Automated Weather Data Network (AWDN) across Nebraska, USA. It should be stressed here that due to the uncertainties associated with each technique for estimating *GR*, it is critical to compare *GR* results from multiple methods (Scanlon et al., 2002). Thus, *GR* estimated from a number of techniques in the study area was used to cross-validate the inverse modeling results. With the aid of existing soil moisture monitoring networks, this study has important implications for aiding water resources management in different regions around the globe.

2. Materials and methods

2.1. Study area and soil moisture data

The study area covers the state of Nebraska with an area of approximately 2.0 × 10^5 km^2 (Fig. 1). The climate in the region is characterized as a continental semiarid type. From western to eastern Nebraska, mean annual precipitation increases from about 35 cm/year to over 75 cm/year (the mean annual precipitation map can be accessed at http://www.hprcc.unl.edu/index.php).

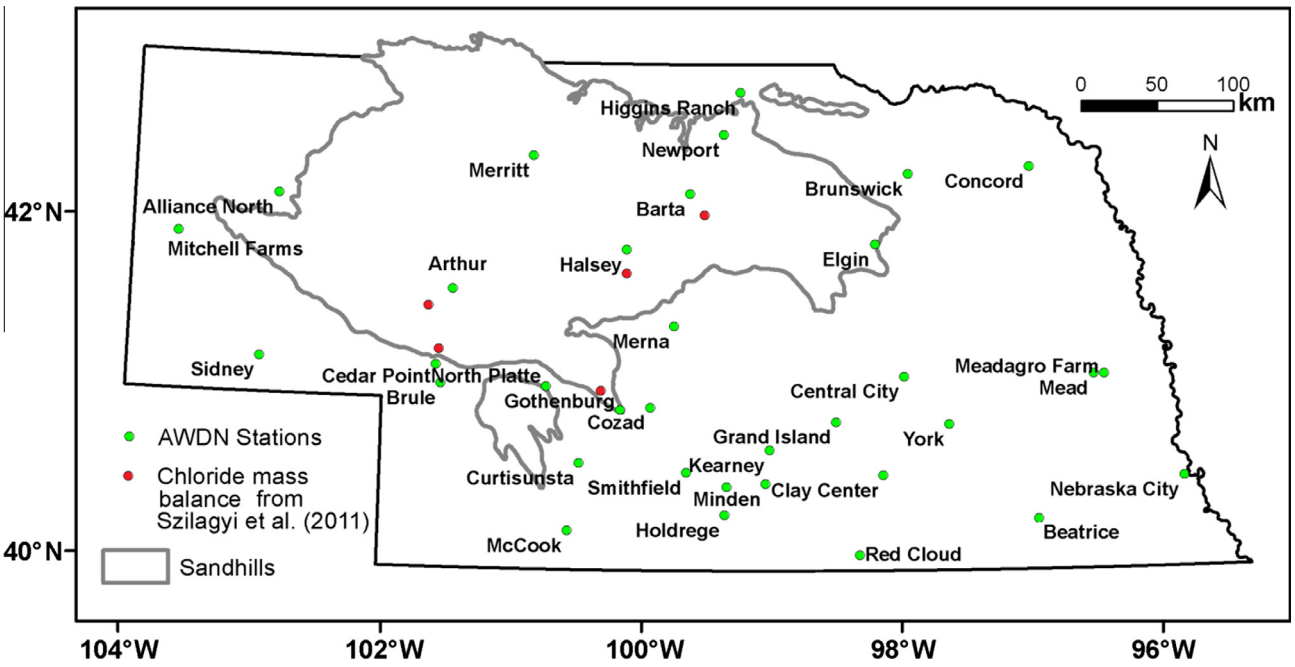

Fig. 1. Location map of soil moisture stations from the Automated Weather Data Network (AWDN) across Nebraska.

The land surface is primarily covered by natural grasses and cultivated crops (Istanbulluoglu et al., 2012). Within the Nebraska Sandhills (Fig. 1), sandy soils are dominant, while finer-textured soils, such as loam and silt loam, are found outside the Nebraska Sandhills (Istanbulluoglu et al., 2012). The infiltration rate across Nebraska varies between ~ 2 cm/day and ~ 790 cm/day (data were retrieved from the State Soil Geographic (STATSGO) dataset at http://www.soilinfo.psu.edu/index.cgi?index.html). In addition, field studies showed that saturated hydraulic conductivities varied from about 110 cm/day to slightly over 2000 cm/day in the eastern Nebraska Sandhills (Wang et al., 2008, 2015d). The sediments across Nebraska are mainly comprised of eolian deposits with sand deposits in the Nebraska Sandhills and loess deposits in central and eastern Nebraska (Mason, 2001; Miao et al., 2007). The thickness of the vadose zone shows significant spatial variations across the region. The depth to water table ranges from several meters to tens of meters at the study sites (see supplemental Table 1S for detailed information). The High Plains Aquifer that primarily consists of sand, gravel, and sandstone underlies about 84% of Nebraska, while local paleovalley, glacial, and recent alluvial aquifers are mainly found in eastern Nebraska (Korus et al., 2013). The average thickness of the High Plains Aquifer in the Nebraska Sandhills is about 182 m, while the thickness of the High Plains Aquifer varies between 30 m and 122 m outside the Nebraska Sandhills. From a hydrological perspective, Nebraska occupies an important place in the water budget of the Great Plains, as the largest portion of groundwater storage in the High Plains Aquifer is found underneath Nebraska's borders with an estimated volume of 2.438×10^3 km^3 or about 68% of the total storage of the High Plains Aquifer (Scanlon et al., 2012). In addition, the Nebraska Sandhills is the largest native grassland-stabilized sand dune area in the Western Hemisphere (Loope and Swinehart, 2000). The high infiltration capacity of sandy soils makes this area an important recharge area for the underlying High Plains Aquifer (Szilagyi et al., 2003, 2011; Wang et al., 2009b; Scanlon et al., 2012). Partly owing to the importance of groundwater resources for agricultural irrigation in Nebraska (Wen and Chen, 2006), it is critical to understand the naturally occurring *GR* across the region for assessing the sustainability of water resources.

In order to use inverse modeling for estimating *GR*, daily soil moisture data at four depths (i.e., 10, 25, 50, and 100 cm) were retrieved from the AWDN stations across Nebraska, which are operated by the High Plains Regional Climate Center at the University of Nebraska. In this study, a total of 34 AWDN stations were selected with daily soil moisture data spanning from 2008 to 2013 (Fig. 1 and Table 1). Those AWDN sites are covered by natural grasses under rainfed conditions with gentle slopes. Hourly soil moisture at the AWDN sites is measured using Theta probes (ML2x sensors, Delta-T Devices, Cambridge, UK) that were calibrated at each site (Hubbard et al., 2009). The hourly moisture data were then integrated to daily values and used in this study. At each AWDN site, hydrometeorological data were also recorded, including precipitation (P), air temperature, radiation, relative humidity, and wind speed. Daily potential evapotranspiration (ET_p) was calculated based on the Penman–Monteith equation (Allen et al., 1998), which was then used along with daily P to drive the VZM.

Table 1
Statistical summary of annual precipitation (P) and potential evapotranspiration (ET_p) at the AWDN stations during the study period from 2000 to 2013.

AWDN station	Latitude	Longitude	P (cm/year)		ET_p (cm/year)	
			Mean	Range (standard deviation)	Mean	Range (standard deviation)
Alliance North	42.18	−102.92	34.49	13.28–54.87 (10.37)	131.64	115.84–155.35 (11.30)
Arthur	41.65	−101.52	44.12	14.63–67.32 (13.68)	130.14	111.61–163.21 (12.98)
Barta	42.23	−99.65	52.44	25.77–70.09 (12.10)	127.15	106.96–157.73 (12.74)
Beatrice	40.30	−96.93	63.11	42.43–106.95 (16.81)	115.41	104.22–137.59 (9.84)
Brule	41.09	−101.59	43.62	14.86–63.61 (11.44)	133.09	120.26–176.78 (14.37)
Brunswick	42.35	−97.92	59.64	27.98–86.42 (13.59)	101.56	86.44–127.16 (9.99)
Cedar Point	41.20	−101.63	41.05	16.90–57.77 (12.21)	125.62	108.01–153.38 (12.06)
Central City	41.15	−97.97	56.68	24.58–99.80 (17.92)	105.84	91.27–123.48 (10.42)
Clay Center	40.57	−98.13	64.43	48.36–90.57 (13.21)	111.81	100.84–134.20 (9.12)
Concord	42.38	−96.95	69.68	49.44–106.17 (16.85)	105.80	92.21–133.68 (10.16)
Cozad	40.97	−99.95	52.49	20.83–74.44 (14.58)	109.95	97.77–137.37 (13.16)
Curtisunsta	40.63	−100.50	47.98	25.18–76.08 (14.05)	128.52	107.76–153.37 (13.26)
Elgin	41.93	−98.18	61.53	34.08–90.43 (16.14)	113.18	96.97–138.75 (11.16)
Gothenburg	40.95	−100.18	51.78	19.70–86.95 (17.42)	123.84	106.13–155.84 (12.35)
Grand Island	40.88	−98.50	51.95	23.34–80.41 (15.24)	114.83	101.82–139.37 (10.08)
Halsey	41.90	−100.15	52.76	28.16–82.03 (13.91)	130.90	111.66–154.05 (11.58)
Higgins Ranch	42.83	−99.25	54.81	35.76–78.92 (12.54)	121.38	102.61–154.15 (14.17)
Holdrege	40.33	−99.37	55.82	32.46–75.30 (13.85)	126.31	110.52–149.49 (11.50)
Holdrege 4n	40.50	−99.35	60.28	34.90–87.46 (14.99)	119.30	102.93–141.14 (11.16)
Kearney	40.72	−99.02	53.75	28.97–82.80 (15.76)	122.92	107.34–148.72 (10.44)
McCook	40.23	−100.58	48.85	29.58–65.34 (12.14)	134.20	113.98–157.88 (13.21)
Mead	41.15	−96.48	67.20	44.04–98.02 (14.76)	108.08	93.61–132.25 (9.87)
Meadagro Farm	41.15	−96.40	65.90	42.63–93.11 (13.96)	103.95	92.24–123.82 (8.78)
Merna	41.45	−99.77	54.46	22.99–83.71 (17.49)	113.30	94.18–142.57 (12.10)
Merritt	42.45	−100.90	48.18	26.97–61.66 (10.83)	125.65	112.09–156.66 (13.36)
Minden	40.52	−99.05	59.09	32.10–85.05 (15.84)	115.91	102.05–134.21 (10.58)
Mitchell Farms	41.93	−103.70	30.62	11.65–44.01 (9.33)	132.15	118.15–158.96 (10.59)
Nebraska City	40.53	−95.80	61.45	46.18–96.36 (12.90)	105.75	93.36–127.19 (10.05)
Newport	42.58	−99.38	57.77	31.76–78.92 (13.51)	116.05	103.05–146.94 (11.48)
North Platte	41.08	−100.77	45.07	18.51–62.16 (14.66)	113.69	98.29–131.20 (9.45)
Red Cloud	40.08	−98.28	58.20	38.86–86.17 (13.28)	122.89	108.76–145.75 (10.38)
Sidney	41.22	−103.02	39.20	21.59–56.30 (11.51)	143.87	123.12–170.04 (13.38)
Smithfield	40.58	−99.67	58.64	30.69–81.88 (14.16)	121.88	105.94–146.86 (11.65)
York	40.87	−97.62	57.89	36.95–81.50 (11.86)	107.34	98.08–126.27 (7.92)

2.2. Model setup and parameterization

The Hydrus-1D model (Šimunek et al., 2013) was adopted for computing *GR*, which is based on the Richards equation for simulating soil moisture dynamics in vadose zones with reasonable accuracy (Zlotnik et al., 2007). At the surface of the modeled soil columns, an atmospheric boundary condition was selected, which could switch from a prescribed flux to a prescribed pressure head when limiting pressure heads were exceeded. Surface runoff was allowed without ponding when the intensity of *P* was higher than soil infiltration capacity or soil became saturated. A free drainage condition was set at the lower boundary. Based on the depth to water table across the study area (Table 1S), the length of the modeled soil columns was 1.5 m with a total of 151 nodes at 1-cm intervals. In this study, naturally occurring *GR* was defined as the amount of water that passed the lower boundary. Vegetated surface conditions were simulated, which required separate inputs of potential evaporation (E_p) and potential transpiration (T_p). To partition ET_p into E_p and T_p, Beer's law was used:

$$E_p(t) = ET_p(t) \times e^{-k \times LAI(t)} \tag{1}$$

$$T_p(t) = ET_p(t) - E_p(t) \tag{2}$$

where k is an extinction coefficient with its value set to be 0.5 and *LAI* is leaf area index [L^2/L^2]. The model of Feddes et al. (1978) was adopted to compute root water uptake $S(h)$:

$$S(h) = \alpha(h) \times S_p \tag{3}$$

where $\alpha(h)$ [–] is a dimensionless function and varies between 0 and 1 depending on soil matric potentials, and S_p [1/T] is the potential root water uptake and assumed to be equal to T_p. The distribution of S_p over the root zone was based on root density distributions. The root water uptake was then assumed to be equal to actual transpiration, and the actual evapotranspiration (ET_a) was the sum of actual soil evaporation and actual transpiration.

To ensure the generality of this study, publicly available data and literature values were used to parameterize the Hydrus-1D model. To partition daily ET_p into E_p and T_p (i.e., Eqs. (1) and (2)), *LAI* data at each AWDN site were obtained from the MODIS_MOD15A2 dataset with a spatial resolution of 1 km and a temporal resolution of 8 days (Myneni et al., 2002). Following the procedure of Wang and Zlotnik (2012), a 3 × 3 cell window (i.e., 3 × 3 km) centered at an AWDN location was used to extract *LAI* data from the MODIS_MOD15A2 dataset. Average *LAI* values were first calculated from the 3 × 3 cell window and then used to obtain daily *LAI* values by linearly interpolating those data. Given that the AWDN sites are covered by natural grasses, the root density distribution was assumed to follow the model in Jackson et al. (1996) for grasses:

$$Y(d) = 1 - \beta^d \tag{4}$$

where Y [–] is the cumulative root fraction and varies between 0 and 1, d [L] is the soil depth in cm, and β is an extinction coefficient with its value of 0.943 for temperate grasslands (Jackson et al., 1996). In addition, the parameter values for delineating root water uptake (i.e., $\alpha(h)$) were taken from the default values for grasses given in the Hydrus-1D model.

2.3. Inverse modeling

For the soil hydraulic functions, the van Genuchten model (Mualem, 1976; van Genuchten, 1980) was adopted:

$$\theta(h) = \begin{cases} \theta_r + \frac{\theta_s - \theta_r}{(1+|\alpha h|^n)^m}, & h < 0 \\ \theta_s, & h \geqslant 0 \end{cases} \tag{5}$$

$$K(S_e) = K_S \times S_e^l \times \left[1 - \left(1 - S_e^{1/m}\right)^m\right]^2 \tag{6}$$

where θ [L^3/L^3] is volumetric moisture content; h [L] is pressure head; θ_r [L^3/L^3] and θ_s [L^3/L^3] are residual and saturated moisture content, respectively; K [L/T] and K_S [L/T] are unsaturated and saturated hydraulic conductivity, respectively; and $S_e = (\theta - \theta_r)/(\theta_s - \theta_r)$ [–] is saturation degree. For the fitting factors, α [1/L] is inversely related to air entry pressure, n [–] measures the pore size distribution of a soil with $m = 1 - 1/n$, and l [–] is a parameter accounting for pore tortuosity and connectivity.

The inversion algorithm implemented in the Hydrus-1D model was used to optimize the van Genuchten parameters listed in Eqs. (5) and (6). Given the availability of soil moisture data at the AWDN sites, the modeled soil columns were divided into four layers (i.e., 0–17.5 cm, 17.5–37.5 cm, 37.5–75.0 cm, and 75.0–150.0 cm), which led to a total of 24 hydraulic parameters. However, the maximum number of parameters that can be optimized by the Hydrus-1D model is 15. Therefore, the optimization procedure used by Turkeltaub et al. (2015) was adopted here. Specifically, the parameters of the upper two layers were first optimized, while the parameters of the remaining lower two layers were fixed. Then, the optimized parameters of the upper two layers were fixed and the parameters of the lower two layers were optimized. This procedure was repeated until there were no further improvements in the optimized parameters or the changes in the lowest sum of squares were less than 0.1%. The parameter bounds used for the optimizations are given in Table 2. Note that for θ_r, the upper bound was reduced to the lowest observed value when it was less than 0.1. The Marquardt–Levenberg nonlinear minimization method employed by the Hydrus-1D model is sensitive to the initial values of the van Genuchten parameters. To resolve this issue, two soil datasets were used to initialize the van Genuchten parameters. First, soil particle size distributions at AWDN sites were retrieved from the global soil database of Shangguan et al. (2014). It was then converted to the van Genuchten parameters using the Rosetta program (Schaap et al., 2001). For the second soil dataset, the van Genuchten parameter values given by Carsel and Parrish (1988) were also adopted as initial values. Based on the regional soil map of Nebraska (Istanbulluoglu et al., 2012), a total of 6 soil textures were considered at each AWDN site, including sand, loamy sand, sandy loam, loam, silt loam, and silt, and the van Genuchten parameter values for those soil textures (Carsel and Parrish, 1988) were then used as initial values.

For all optimizations, the initial soil moisture profile at each AWDN site was set to the observed moisture data on January 1, 2008. A period of one year (i.e., the year of 2008) was used as a spin-up period to minimize the effect of initial conditions. The calibration and validation periods were from 2009 to 2011 and 2012 to 2013, respectively. For the goodness-of-fit assessment, three performance criteria were selected to evaluate the model results, including Average Error (AE), Root Mean Square Error (RMSE), and Nash–Sutcliffe Efficiency (NSE):

$$\mathrm{AE} = \frac{\sum_{i=1}^{n}(S_i - O_i)}{n} \tag{7}$$

$$\mathrm{RMSE} = \sqrt{\frac{1}{n}\sum_{i=1}^{n}(S_i - O_i)^2} \tag{8}$$

Table 2
Bounds of the van Genuchten parameters used for inverse calculations.

	θ_r (–)	θ_s (–)	α (1/cm)	n (–)	K_S (cm/day)	l (–)
Range	0–0.1	0.3–0.5	0.001–0.2	1.1–4.0	1–2000	−1 to 1

$$\mathrm{NSE} = 1 - \frac{\sum_{i=1}^{n}(S_i - O_i)^2}{\sum_{i=1}^{n}(O_i - \overline{O_i})^2} \quad (9)$$

where n is the total number of data points of soil moisture, and S_i and O_i are the simulated and observed daily soil moisture content on day i, respectively. The NSE has been widely used to assess the predictive power of hydrological models with its value of 1 indicating a perfect match between modeled and observed data (Nash and Sutcliffe, 1970). In order to cross-validate *GR* estimates using auxiliary datasets, after the optimizations, *GR* was recalculated at each AWDN site from 2001 to 2013 with the year of 2000 as the spin-up period, based on the optimized parameter set of the highest NSE score.

3. Results and discussion

3.1. Hydroclimatic conditions

An overview of the hydroclimatic conditions across the study area is given as a statistical summary of annual P and ET_p at each AWDN site in Table 1. Fig. 2 illustrates the longitudinal dependence of mean annual P ($\overline{P}$; overbars denote mean annual values hereafter) and $\overline{ET_p}$ across Nebraska. Fig. 2 reveals the existence of a strong $\overline{P}$ gradient across the study area, increasing from 30.62 cm/year at Mitchell Farms in western Nebraska to 69.68 cm/year at Concord in eastern Nebraska. In contrast, $\overline{ET_p}$ showed an opposite spatial trend, which decreased from ~140 cm/year in western Nebraska to ~100 cm/year in eastern Nebraska. On annual time scales, there also existed significant interannual variability in P at all the AWDN sites. During the study period from 2000 to 2013, annual P at the AWDN sites (except for at Clay Center) varied by a factor greater than 2. By comparison, the interannual variability in ET_p was still significant, but to a lesser degree. In addition, with increasing $\overline{P}$ and $\overline{ET_p}$, the variability in annual P and ET_p also increased, as indicated by the standard deviations shown in Fig. 2. Partly due to the significant variability in P and ET_p, *GR* exhibited considerable spatial variations across Nebraska (Szilagyi and Jozsa, 2013), making the study area ideal for assessing the feasibility of using inverse vadose zone modeling for estimating *GR* from large-scale soil moisture monitoring networks.

3.2. Temporal evolution of soil moisture

Due to the large number of the AWDN sites, only the mean ($\bar{\theta}$) and standard deviation (σ_θ) of daily soil moisture contents, which were derived from the soil moisture data of all the AWDN sites, are plotted in Fig. 3. The seasonality of the observed $\bar{\theta}$ was obvious at all the depths. With decreasing depths, the temporal dynamics of $\bar{\theta}$ also became stronger, mostly because of the tighter coupling between soil moisture and land surface processes at shallower soil depths (Martinez-Fernandez and Ceballos, 2003; Guber et al., 2008; Wang et al., 2015b). More importantly, σ_θ in Fig. 3 reveals that soil moisture varied considerably across the AWDN sites. In addition to the effects of climatic conditions, soil moisture levels were largely controlled by soil properties at the study sites (Mahmood et al., 2012; Wang et al., 2015c). For example, Mahmood et al. (2012) analyzed soil moisture data from AWDN stations from eastern to western Nebraska and found that sandy soils generally had lower soil moisture levels than silty soils.

As another demonstration, observed daily soil moisture contents from Mitchell Farms, Barta, and Concord with similar latitudes are plotted in Figs. 4, 5 and 6, respectively. Barta resides within the Nebraska Sandhills with the dominant soil texture of sand, while Mitchell Farms and Concord are located outside the Nebraska Sandhills with finer-textured soils (Fig. 1). Despite the much drier climatic conditions at Mitchell Farms ($\overline{P} = 30.62$ cm/year and $\overline{ET_p} = 132.15$ cm/year), soil moisture levels at Barta ($\overline{P} = 52.44$ cm/year and $\overline{ET_p} = 127.15$ cm/year) were consistently lower, due to less water holding capacities of sandy soils. With the wettest climate ($\overline{P} = 69.68$ cm/year and $\overline{ET_p} = 105.80$ cm/year) and finer soils at Concord, soil moisture levels were considerably higher than the ones at the other two sites.

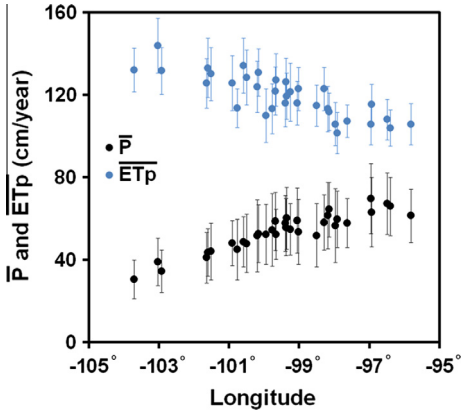

Fig. 2. Dependence of mean annual precipitation ($\overline{P}$) and mean annual potential evapotranspiration ($\overline{ET_p}$) on longitudes at AWDN sites. Data from 2000 to 2013 were used to calculate $\overline{P}$ and $\overline{ET_p}$, and vertical bars represent one standard deviation.

3.3. Results from inverse modeling

Daily soil moisture data from 2009 to 2011 and from 2012 to 2013 were used for calibration and validation, respectively. Note that compared with previous studies (e.g., Jiménez-Martínez et al., 2009; Lu et al., 2011; Min et al., 2015; Ries et al., 2015; Turkeltaub et al., 2015), the time series of soil moisture data used for calibration and validation were noticeably longer in this study. Both wet (e.g., 2011) and dry (e.g., 2012) years were encountered during the simulation period (Figs. 4–6). For the goodness-of-fit assessment, the resulting values of AE, RMSE, and NSE are reported in Table 3 for the calibration period and in Table 4 for the validation period.

It is important to notice that even though no detailed information on local conditions was utilized to parameterize the Hydrus-1D model, the obtained RMSE values during the calibration period fell within the general ranges of RMSE reported by previous studies (e.g., Jiménez-Martínez et al., 2009; Assefa and Woodbury, 2013; Min et al., 2015). These results demonstrated the applicability of the procedure used for model parameterizations in the study area. In particular, with decreasing depths, the RMSE values tended to be smaller, most likely due to the less temporal variations in soil moisture at deeper soil depths (Fig. 3). The values of AE during the calibration period were generally close to zero, indicating that the simulated long-term soil water storage matched well with the observed ones. More interestingly, compared to AE and RMSE, the differences in the NSE values were more contrasting among the sites, suggesting that the use of NSE might be better for evaluating model performances; however, this topic is beyond the scope of this study but deserves further investigation. The model performances were less successful during the validation period, probably due to the record drought conditions in 2012. For instance, the formations of soil crusts under extreme drought conditions might alter the infiltration and evaporation processes (Abu-Awwad,

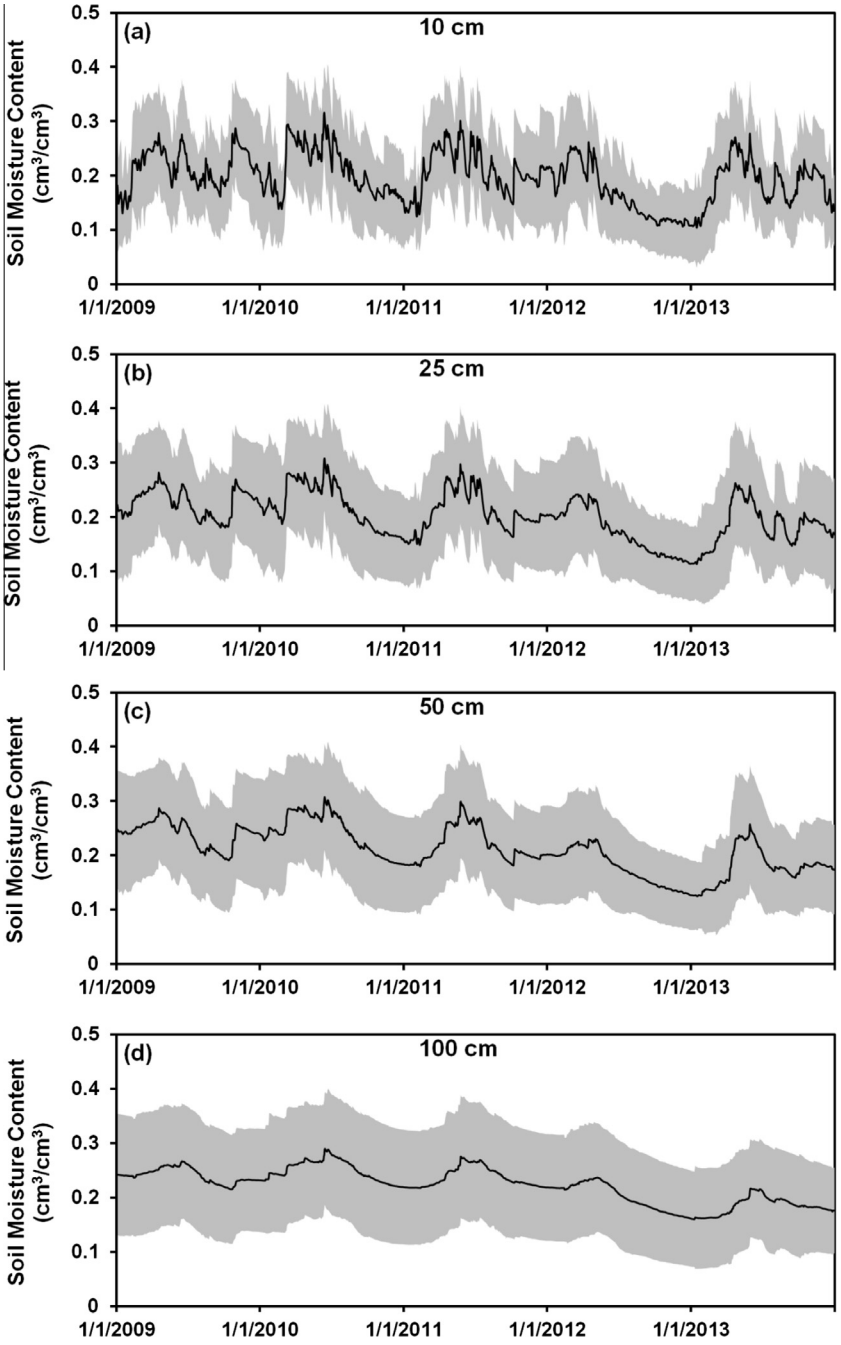

Fig. 3. Temporal evolutions of daily soil moisture contents at different soil depths. The black lines represent daily mean soil moisture contents calculated from all AWDN stations and the gray areas indicate one standard deviation.

1997; Al-Kaisi et al., 2013), as indicated by the larger deteriorations of the model performances during the validation period at the AWDN sites with drier climatic conditions and finer-textured soils.

Examples of observed and simulated daily soil moisture contents along with daily meteorological data are plotted in Figs. 4–6 for Mitchell Farms, Barta, and Concord with different climatic and soil conditions. For the purpose of brevity, only the optimized van Genuchten parameters for the above three sites are reported in Table 5 (the rest of the optimized parameters can be found in the supplemental Table 2S) along with the sand percent from Shangguan et al. (2014). For the optimized K_S, it tended to increase with increasing sand percent. For instance, the optimized K_S was generally higher at Barta, which was also consistent with field measurements of K_S at Barta (Wang et al., 2015d); whereas, the optimized K_S was lowest at Concord. As expected, with increasing annual P (i.e., from Mitchell Farms, Barta to Concord), soil moisture showed stronger temporal dynamics, due to the larger number of precipitation events. Overall, the simulated soil moisture contents corresponded well with the inputs of P, and were able to capture most of the observed soil moisture peaks as well as drainage processes. However, some of the observed soil moisture peaks were missed by the simulations (e.g., in September and October 2010 at Mitchell Farms, and April 2009 at Concord), because of the insufficient model inputs of P (see Figs. 4 and 6). Although the reasons for the mismatches between the recorded P (i.e., model inputs)

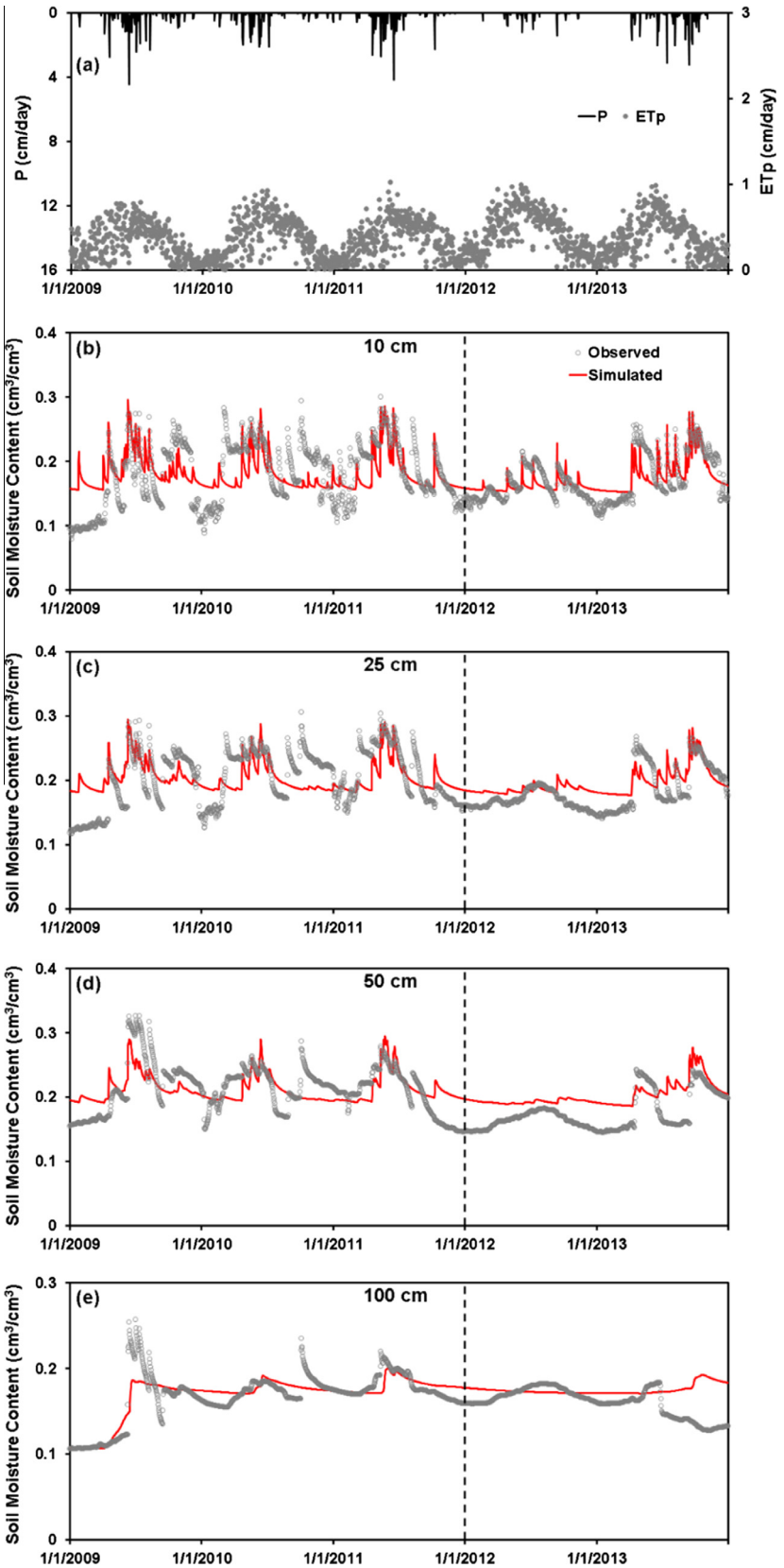

Fig. 4. Daily precipitation (P) and potential evapotranspiration (EP_p), and observed and simulated soil moisture contents during the calibration (2009–2011) and validation (2012–2013) periods at Mitchell Farms.

and the observed soil moisture contents were unknown, it would clearly cause the deviations of the simulated soil moisture contents from the observed ones.

In addition to the uncertainties in the observed soil moisture data and/or model inputs, other reasons might also contribute to the deviations between observed and simulated soil moisture

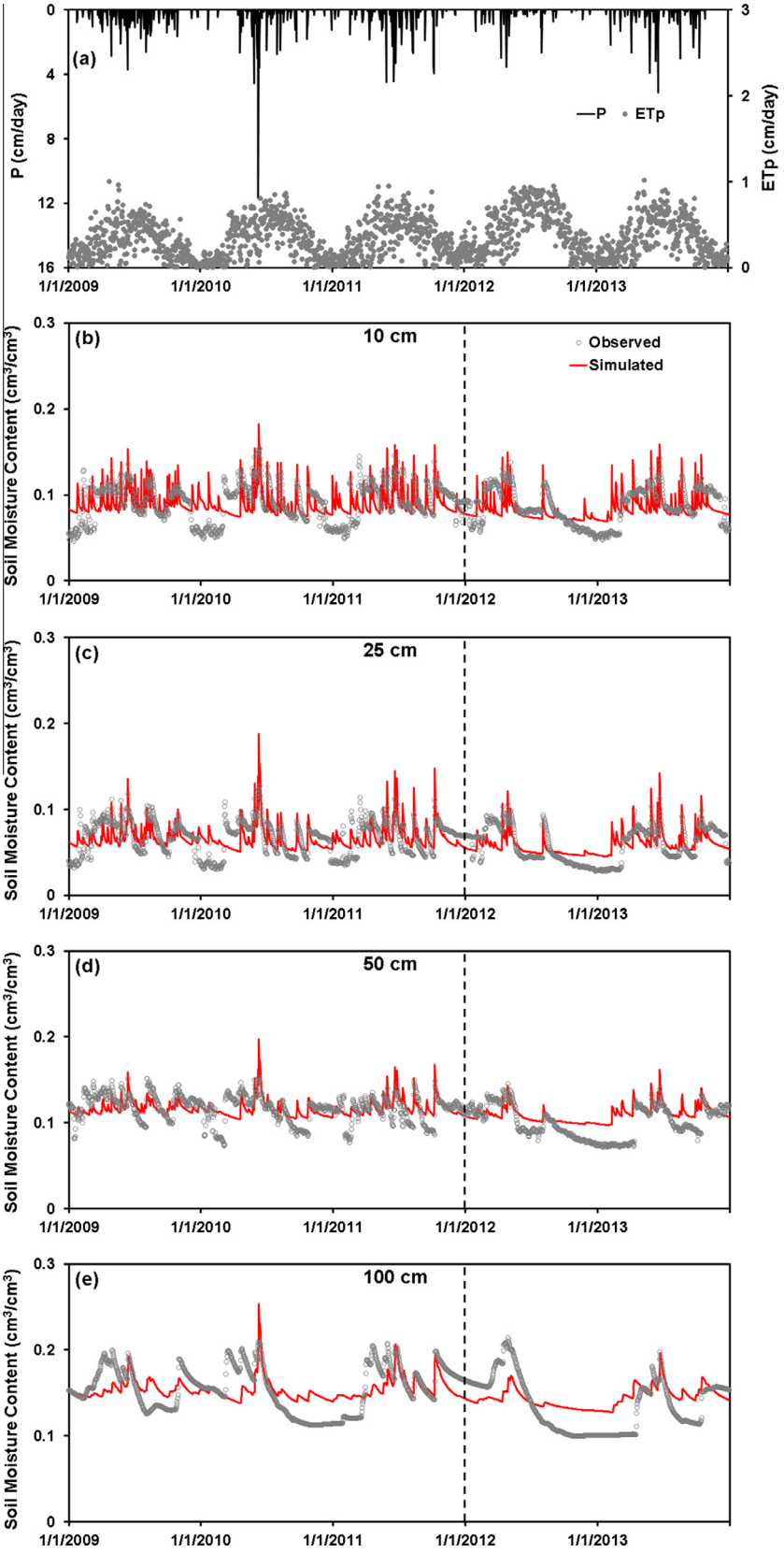

Fig. 5. Daily precipitation (P) and potential evapotranspiration (EP_p), and observed and simulated soil moisture contents during the calibration (2009–2011) and validation (2012–2013) periods at Barta.

contents (e.g., macropore flow, lateral flux of soil moisture, and shallow groundwater), which were not considered in this study. For instance, previous studies showed that shallow groundwater could affect soil moisture dynamics, land surface processes, and groundwater recharge (Maxwell and Kollet, 2008; Wang et al., 2009a; Soylu et al., 2011; Brunner et al., 2012). In particular,

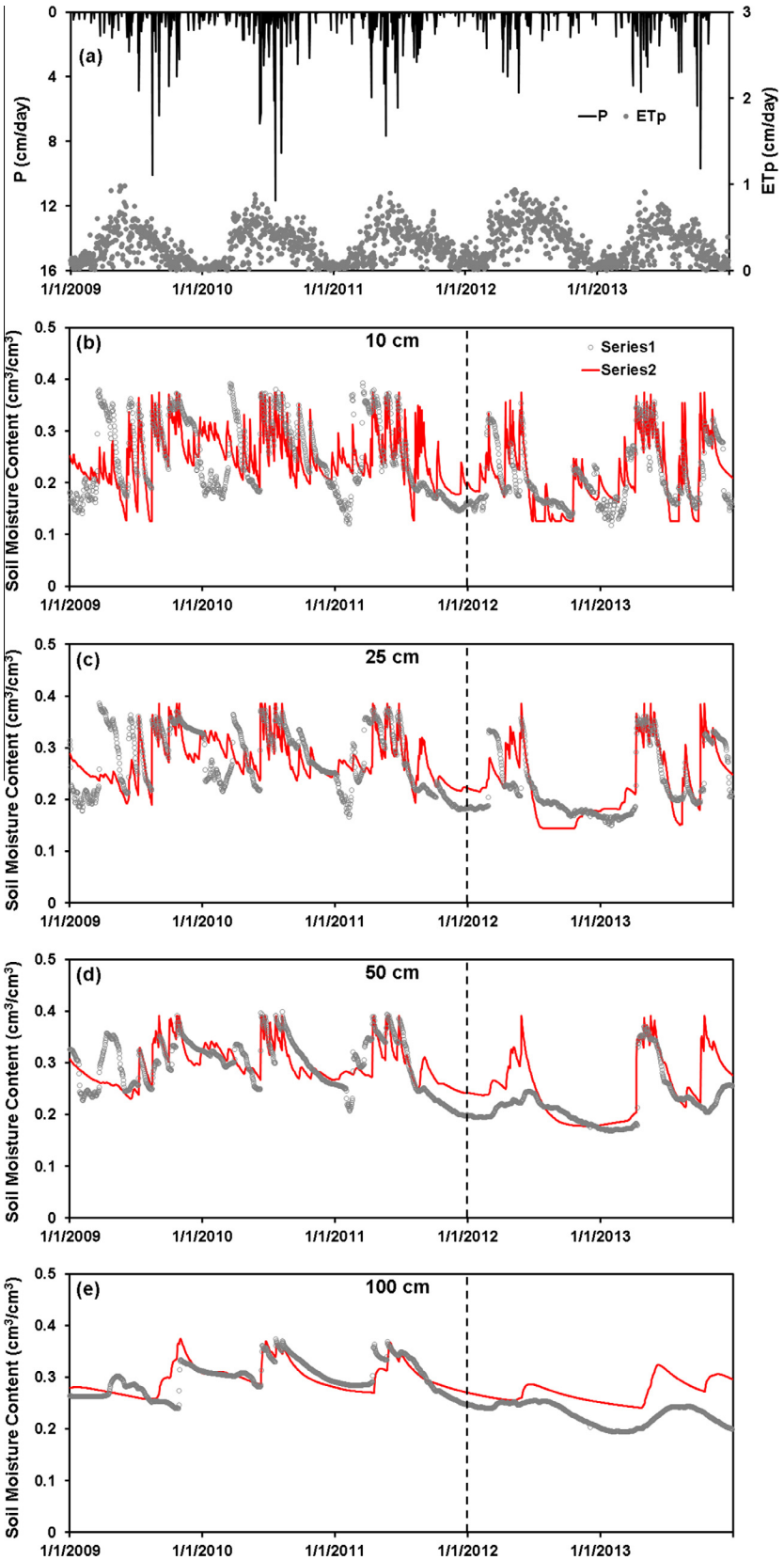

Fig. 6. Daily precipitation (P) and potential evapotranspiration (EP_p), and observed and simulated soil moisture contents during the calibration (2009–2011) and validation (2012–2013) periods at Concord.

Brunner et al. (2012) pointed out that the use of soil moisture data for calibrating groundwater and vadose zone models was heavily dependent on the depth to water table. There were no groundwater level measurements made at the AWDN sites. To resolve this issue, data on the average depth to water table from 2008 to 2013 were obtained from nearby observational

Table 3
Goodness-of-fit measures for simulated and observed soil moisture data at different depths during the calibration period from 2009 to 2011.

AWDN station	Average Error (AE)				Root Mean Square Error (RMSE)				Nash–Sutcliffe Efficiency (NSE)			
	10 cm	25 cm	50 cm	100 cm	10 cm	25 cm	50 cm	100 cm	10 cm	25 cm	50 cm	100 cm
Alliance North	−0.001	0.001	−0.004	−0.005	0.053	0.047	0.057	0.021	0.309	0.347	0.244	0.284
Arthur	0.001	0.000	0.000	0.000	0.032	0.026	0.033	0.014	0.327	0.449	0.413	0.341
Barta	−0.001	0.000	0.000	−0.001	0.021	0.018	0.015	0.023	0.047	0.165	0.092	0.254
Beatrice	−0.002	−0.001	−0.004	−0.001	0.071	0.050	0.064	0.022	0.191	0.337	0.360	0.381
Brule	−0.003	−0.001	0.000	0.001	0.066	0.047	0.029	0.025	0.323	0.289	0.453	0.495
Brunswick	0.000	0.000	0.000	−0.002	0.058	0.043	0.033	0.030	0.231	0.435	0.643	0.351
Cedar Point	0.000	−0.001	−0.001	0.000	0.044	0.033	0.038	0.012	0.322	0.535	0.400	0.359
Central City	−0.001	−0.002	−0.001	0.000	0.057	0.035	0.026	0.056	0.467	0.587	0.470	0.169
Clay Center	−0.005	−0.004	0.000	0.002	0.062	0.068	0.095	0.038	0.154	0.424	0.258	0.289
Concord	−0.003	−0.002	0.000	0.000	0.064	0.050	0.036	0.023	0.219	0.302	0.465	0.497
Cozad	0.000	−0.001	−0.008	−0.015	0.077	0.047	0.051	0.023	0.267	0.464	0.529	−0.007
Curtisunsta	−0.005	−0.021	−0.033	−0.031	0.049	0.060	0.057	0.040	0.348	0.401	−0.059	−1.440
Elgin	0.000	0.000	0.001	0.000	0.037	0.029	0.041	0.020	0.338	0.374	0.205	0.443
Gothenburg	−0.001	0.000	0.000	0.000	0.024	0.016	0.019	0.038	0.101	0.237	0.451	0.426
Grand Island	0.000	0.000	−0.001	0.000	0.057	0.046	0.023	0.015	0.267	0.231	0.427	−0.102
Halsey	0.000	0.000	0.000	0.000	0.026	0.024	0.016	0.018	0.214	0.304	0.289	0.068
Higgins Ranch	0.000	0.000	0.000	0.000	0.024	0.017	0.012	0.007	0.193	0.307	0.352	0.416
Holdrege	0.000	0.001	−0.005	−0.002	0.059	0.040	0.052	0.034	0.172	0.471	0.410	0.127
Holdrege 4n	−0.001	0.000	0.000	−0.001	0.039	0.029	0.045	0.046	0.339	0.452	0.392	0.274
Kearney	0.000	0.001	−0.001	0.000	0.046	0.033	0.036	0.025	0.330	0.575	0.715	0.206
McCook	0.000	−0.001	0.000	−0.002	0.047	0.037	0.041	0.014	0.308	0.397	0.399	0.344
Mead	0.002	0.003	−0.001	0.000	0.051	0.032	0.033	0.024	0.186	0.322	0.194	0.245
Meadagro Farm	0.000	0.000	0.000	−0.001	0.052	0.037	0.045	0.019	0.240	0.361	0.347	0.308
Merna	0.001	0.001	0.001	−0.001	0.038	0.039	0.039	0.013	0.385	0.419	0.047	0.059
Merritt	0.000	0.000	0.000	0.000	0.039	0.029	0.017	0.018	0.209	0.372	0.472	0.426
Minden	0.000	−0.001	0.000	−0.001	0.065	0.062	0.046	0.040	0.033	0.203	0.267	0.090
Mitchell Farms	0.000	0.000	0.000	0.001	0.042	0.038	0.030	0.015	0.274	0.262	0.372	0.711
Nebraska City	−0.001	0.000	0.000	−0.001	0.072	0.067	0.077	0.025	0.033	0.064	−0.017	−0.166
Newport	−0.003	−0.001	0.004	0.000	0.025	0.026	0.057	0.011	0.590	0.708	0.309	−0.088
North Platte	0.000	0.000	0.001	−0.001	0.041	0.035	0.042	0.029	0.382	0.651	0.526	0.075
Red Cloud	−0.001	−0.004	−0.001	0.000	0.063	0.068	0.043	0.042	0.247	0.468	0.447	0.308
Sidney	0.000	−0.001	0.000	0.000	0.047	0.034	0.037	0.009	0.498	0.685	0.367	0.679
Smithfield	0.000	−0.001	−0.001	−0.001	0.058	0.037	0.018	0.013	0.248	0.562	0.680	0.556
York	0.000	0.000	0.000	0.000	0.048	0.043	0.008	0.007	0.201	0.369	0.323	−0.683

groundwater wells operated by the USGS Active Groundwater Level Network (http://groundwaterwatch.usgs.gov/default.asp; see supplemental Table 1S for detailed information). Although the depth to water table was deeper than 1.5 m at all the sites, water table could approach the depth of the lower boundary of the model (i.e., 1.5 m) at some locations. For example, the average depth to water table was 2.4 m at Nebraska City. It could explain the poorer model performance at Nebraska City (Table 3), indicating that the free drainage lower boundary condition might not be valid at this site. Nevertheless, with only the aid of publicly available data and literature values for parameterizing the Hydrus-1D model, the inverse modeling results of this study were generally comparable to the ones of previous studies.

3.4. Comparisons of GR and ET_a estimates from inverse modeling with other techniques

The calibrated models were used to compute *GR* from 2001 to 2013 at each AWDN site with the year of 2000 as the spin-up period. The summary of the resulting *GR* and ET_a values are given in Table 6. The obtained $\overline{GR}$ values varied by over three orders of magnitude, ranging from <0.01 cm/year at Mitchell Farms to 16.13 cm/year at Higgins Ranch. In addition, significant interannual variability in *GR* also existed at each AWDN site, mainly due to the variations in annual *P* and ET_p. Similar observations can be also made for ET_a with $\overline{ET_a}$ varying from 29.65 cm/year at Mitchell Farms to 60.54 cm/year at Beatrice. The spatial variations in *GR* and ET_a across the sites reflected the differences in local climatic, soil, and vegetation conditions. As pointed out by Scanlon et al. (2002), uncertainties exist for all the available techniques for estimating *GR*. It is thus crucial to evaluate the reliability of *GR* estimates using multiple techniques. In the following sections, the estimates of *GR* and ET_a from the simulations are compared to the results obtained from other techniques, including remotely sensed data, tracer-based approaches, and regional water balance methods.

3.4.1. Comparisons with remotely sensed data

Although ET_a is usually the larger water balance component than *GR* in hydrological cycles, the majority of previous studies only tested model results using observed soil moisture data and/or *GR* estimated from other techniques. Only a few studies attempted to verify model results with measured ET_a (Andreasen et al., 2013; Min et al., 2015), owing to the high costs associated with direct measurements of ET_a (e.g., lysimeter, eddy covariance, and Bowen ratio methods). Meanwhile, the use of remotely sensed products for various hydrological applications has drawn growing interests from different scientific communities (Becker, 2006; Kerr, 2007; Kalma et al., 2008). Based on MODIS and global meteorological data, Mu et al. (2007) developed a global terrestrial evapotranspiration dataset, which was later improved by Mu et al. (2011) (i.e., MODIS_MOD16). The MODIS_MOD16 dataset provides ET_a estimates at a spatial resolution of 1 km and a temporal resolution of 8 days. The same procedure for extracting the MODIS *LAI* data was used to retrieve ET_a from the MODIS_MOD16 dataset at each AWDN site. Fig. 7 compares $\overline{ET_a}$ obtained from the MODIS_MOD16 dataset (denoted as $\overline{ET_a}$-MODIS) and $\overline{ET_a}$ calculated by the calibrated models (denoted as $\overline{ET_a}$-Hydrus) during the period from 2001 to 2013. It can be seen from Fig. 7 that $\overline{ET_a}$-MODIS tended to be smaller than $\overline{ET_a}$-Hydrus. On average, the difference between $\overline{ET_a}$-Hydrus and $\overline{ET_a}$-MODIS was 3.78 cm/year

Table 4
Goodness-of-fit measures for simulated and observed soil moisture data at different depths during the validation period from 2012 to 2013.

AWDN station	Average Error (AE)				Root Mean Square Error (RMSE)				Nash–Sutcliffe Efficiency (NSE)			
	10 cm	25 cm	50 cm	100 cm	10 cm	25 cm	50 cm	100 cm	10 cm	25 cm	50 cm	100 cm
Alliance North	0.008	0.008	0.007	−0.019	0.044	0.043	0.061	0.023	0.463	0.511	0.142	−3.018
Arthur	0.013	0.010	0.019	0.055	0.030	0.026	0.031	0.066	0.228	0.232	0.213	−2.072
Barta	−0.003	0.001	0.010	0.009	0.019	0.016	0.018	0.027	0.180	0.368	0.017	0.247
Beatrice	−0.009	−0.045	−0.048	−0.005	0.078	0.063	0.062	0.040	0.244	0.097	0.130	0.160
Brule	0.030	0.012	0.007	0.019	0.074	0.062	0.034	0.021	0.077	−0.004	−0.281	−1.855
Brunswick	0.002	−0.033	−0.013	0.068	0.047	0.047	0.031	0.079	0.390	0.259	0.456	−1.260
Cedar Point	0.023	0.021	0.028	0.010	0.051	0.039	0.036	0.012	0.292	0.063	−0.281	−1.303
Central City	0.016	−0.007	0.019	0.013	0.054	0.042	0.037	0.053	0.476	0.652	0.458	−0.670
Clay Center	0.002	−0.014	0.018	0.018	0.067	0.078	0.093	0.037	0.115	0.170	0.117	−0.004
Concord	0.002	0.003	0.029	0.045	0.047	0.041	0.050	0.051	0.390	0.538	−0.200	−5.383
Cozad	0.022	0.002	−0.005	0.013	0.066	0.040	0.032	0.019	0.217	0.241	−0.022	0.018
Curtisunsta	0.014	0.015	0.000	0.026	0.060	0.060	0.041	0.030	0.369	0.413	−0.018	−2.348
Elgin	−0.001	0.006	0.000	−0.024	0.033	0.030	0.029	0.038	0.524	0.319	−0.281	0.092
Gothenburg	0.000	−0.006	−0.002	0.054	0.023	0.017	0.018	0.060	0.375	0.585	0.754	−1.386
Grand Island	0.042	0.075	0.054	0.068	0.088	0.108	0.084	0.079	−0.406	−1.068	−0.666	−2.093
Halsey	0.004	0.017	0.008	0.009	0.025	0.030	0.023	0.023	0.383	0.037	0.157	−0.056
Higgins Ranch	0.017	0.007	0.009	0.001	0.025	0.021	0.020	0.012	−0.321	0.278	0.021	0.317
Holdrege	0.034	−0.002	0.061	0.064	0.073	0.051	0.111	0.076	−0.040	0.606	−0.055	−1.936
Holdrege 4n	−0.022	0.002	0.020	0.032	0.045	0.028	0.049	0.043	0.182	0.558	0.228	−0.437
Kearney	0.001	−0.017	−0.030	0.037	0.045	0.043	0.058	0.043	0.461	0.507	0.384	−0.937
McCook	0.064	0.064	0.111	0.082	0.097	0.097	0.124	0.098	−0.613	−0.800	−3.706	−2.267
Mead	0.053	0.045	0.054	0.041	0.087	0.070	0.080	0.053	−0.126	0.083	−0.163	−0.648
Meadagro Farm	−0.012	0.001	0.055	0.021	0.049	0.039	0.070	0.032	0.402	0.564	−0.304	−0.603
Merna	0.006	0.023	0.052	0.029	0.032	0.043	0.062	0.031	0.504	0.465	−0.964	−3.819
Merritt	0.002	0.001	−0.002	0.002	0.030	0.027	0.021	0.025	0.240	0.458	0.492	0.409
Minden	0.042	0.029	0.016	0.023	0.081	0.072	0.033	0.025	−0.321	−0.082	−0.311	−16.982
Mitchell Farms	0.000	0.013	0.028	0.014	0.024	0.025	0.035	0.025	0.509	0.327	−0.567	−1.432
Nebraska City	0.043	−0.032	−0.085	0.007	0.090	0.073	0.092	0.015	−0.179	0.062	−4.694	−0.608
Newport	0.024	0.012	0.059	0.061	0.033	0.024	0.073	0.082	−0.636	0.208	−1.077	−2.946
North Platte	−0.003	−0.003	0.010	0.031	0.033	0.029	0.020	0.043	0.345	0.304	−1.393	−0.906
Red Cloud	0.008	0.002	0.032	0.021	0.076	0.053	0.045	0.031	0.083	0.346	−0.216	0.061
Sidney	0.000	0.001	−0.009	−0.002	0.041	0.028	0.022	0.012	0.531	0.748	0.644	−0.684
Smithfield	0.036	0.041	0.049	0.039	0.073	0.066	0.063	0.045	−0.064	−0.255	−4.540	−3.026
York	−0.006	0.001	0.007	−0.001	0.051	0.053	0.019	0.007	0.132	0.220	0.050	−0.243

Table 5
Optimized van Genuchten parameters for Mitchell Farms, Barta, and Concord, and the sand percent at those sites from Shangguan et al. (2014).

AWDN site	Depth (cm)	θ_r (−)	θ_s (−)	α (1/cm)	n (−)	K_S (cm/day)	l (−)	Sand (%)
Mitchell Farms	0–17.5	0.032	0.364	0.003	1.181	52.1	0.998	67
	17.5–37.5	0.075	0.326	0.001	1.202	1972.0	0.573	60
	37.5–75.0	0.099	0.337	0.001	1.236	2.4	0.978	25
	75.0–150.0	0.087	0.331	0.157	1.120	2000.0	1.000	44
Barta	0–17.5	0.030	0.300	0.084	1.267	2000.0	0.000	87
	17.5–37.5	0.022	0.300	0.017	1.467	2000.0	−0.001	89
	37.5–75.0	0.061	0.300	0.031	1.326	2000.0	0.001	94
	75.0–150.0	0.099	0.306	0.004	1.543	304.6	1.000	95
Concord	0–17.5	0.100	0.375	0.021	1.465	4.2	1.000	8
	17.5–37.5	0.100	0.385	0.022	1.362	3.3	0.002	8
	37.5–75.0	0.001	0.391	0.025	1.183	1.0	0.000	7
	75.0–150.0	0.010	0.449	0.001	1.330	13.7	0.000	8

for all the AWDN sites. At the majority of the AWDN sites, the differences between $\overline{ET_a}$-Hydrus and $\overline{ET_a}$-MODIS were less than 20%. By comparison, the measurement error of ET_a ranges from 10% to 30% (Allen et al., 2011). A number of reasons could be attributed to the discrepancy between $\overline{ET_a}$-Hydrus and $\overline{ET_a}$-MODIS, such as the mismatch of the spatial scales between the two datasets, the uncertainties in the model inputs and inverse modeling, and the uncertainties in the MODIS ET_a algorithm (Mu et al., 2011; Trambauer et al., 2014). Nonetheless, for areas without direct measurements of ET_a or GR estimated from other techniques, the MODIS_MOD16 dataset might provide additional information for cross-validating the water balance components from model results.

Szilagyi et al. (2011) developed a net GR map for the Nebraska Sandhills at the spatial resolution of 1 km, based on the residuals between P (derived from the Parameter-elevation Regressions on Independent Slopes Model-PRISM) and ET_a (derived from linear transformations of the MODIS daytime land-surface temperatures and ancillary meteorological data). Szilagyi and Jozsa (2013) extended their earlier work and mapped net GR for the entire state of Nebraska. The net $\overline{GR}$ during the period from 2000 to 2009 was retrieved from Szilagyi and Jozsa (2013) (denoted as $\overline{GR}$-Szilagyi). Fig. 8 shows the comparison between $\overline{GR}$-Szilagyi and the simulation results (denoted as $\overline{GR}$-Hydrus). Note that $\overline{GR}$ from 2001 to 2009 was used to compute $\overline{GR}$-Hydrus in Fig. 8. Negative values of $\overline{GR}$-Szilagyi in Fig. 8 occurred in western Nebraska. Due to the use of the residual approach for calculating GR, Szilagyi and Jozsa (2013) attributed those negative $\overline{GR}$ values primarily to irrigation

Table 6
Summary of calculated groundwater recharge (GR) and actual evapotranspiration (ET_a) during the period from 2001 to 2013 from the calibrated models.

AWDN stations	$\overline{GR}$[a] (cm/year)	σ_{GR}[b] (cm/year)	$\overline{ET_a}$ (cm/year)	σ_{ETa} (cm/year)	$\overline{GR}/\overline{P}$ (%)
Alliance North	0.08	0.29	32.79	9.28	0.22
Arthur	11.26	6.50	32.74	8.37	25.27
Barta	7.04	5.99	44.72	8.20	13.41
Beatrice	4.30	5.98	60.54	9.19	6.74
Brule	0.42	0.28	42.55	8.68	0.99
Brunswick	2.22	2.29	58.37	9.55	3.68
Cedar Point	2.17	3.11	38.85	9.77	5.18
Central City	2.35	3.29	50.48	8.66	4.05
Clay Center	8.15	5.94	55.86	7.64	12.79
Concord	8.53	8.73	56.58	5.76	12.02
Cozad	1.53	1.09	47.80	11.06	2.89
Curtisunsta	<0.01	<0.01	43.86	9.80	<0.1
Elgin	14.42	10.94	48.16	6.38	23.13
Gothenburg	8.29	9.53	43.80	9.26	15.95
Grand Island	0.03	0.09	47.27	11.29	0.05
Halsey	3.77	6.55	48.26	10.20	7.06
Higgins Ranch	16.13	7.11	39.01	6.58	29.06
Holdrege	4.26	3.10	46.15	8.18	7.58
Holdrege 4n	0.78	0.91	59.61	12.70	1.28
Kearney	0.48	0.48	51.39	9.38	0.89
Mccook	4.35	2.49	41.75	7.90	8.77
Mead	11.91	9.61	47.19	3.42	17.89
Meadagro Farm	2.31	3.45	54.67	5.29	3.41
Merna	10.89	10.78	43.50	10.06	20.00
Merritt	5.39	4.19	41.95	7.71	11.21
Minden	4.85	4.52	45.86	7.22	8.37
Mitchell Farms	<0.01	<0.01	29.65	8.96	<0.1
Nebraska City	13.63	6.02	36.60	4.30	22.10
Newport	5.58	1.91	53.26	10.86	9.50
North Platte	3.30	2.67	40.19	11.16	7.25
Red Cloud	5.21	3.21	53.41	7.41	8.87
Sidney	1.89	2.22	36.64	9.03	4.77
Smithfield	8.65	6.24	49.95	8.09	14.52
York	7.75	3.84	45.31	6.41	13.23

[a] Overbar denotes mean annual values.
[b] σ: standard deviation.

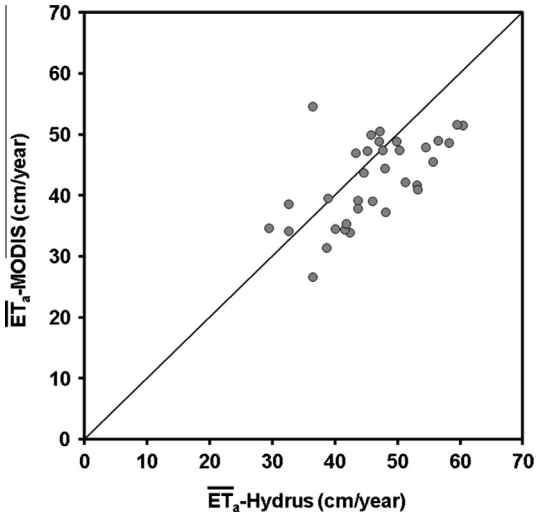

Fig. 7. Comparison between mean annual actual evapotranspiration ($\overline{ET_a}$) calculated by the Hydrus-1D model ($\overline{ET_a}$-Hydrus) and extracted from the MODIS_MOD16 dataset ($\overline{ET_a}$-MODIS) during the period from 2001 to 2013 at all AWDN sites.

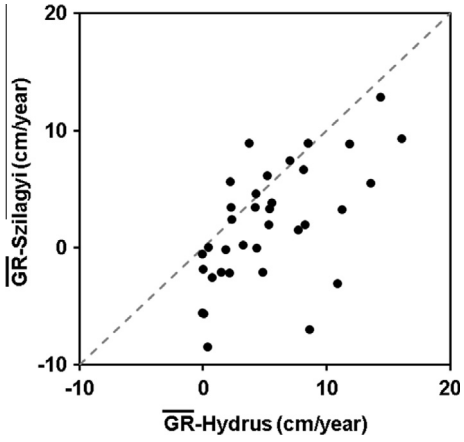

Fig. 8. Comparison between mean annual groundwater recharge ($\overline{GR}$) calculated by the Hydrus-1D model during the period from 2001 to 2009 ($\overline{GR}$-Hydrus) and extracted from Szilagyi and Jozsa (2013) during the period from 2000 to 2009 ($\overline{GR}$-Szilagyi) at all AWDN sites.

in western Nebraska, although no irrigation was allowed at the AWDN stations. Despite those negative values, $\overline{GR}$-Szilagyi was generally comparable to $\overline{GR}$-Hydrus. On average, $\overline{GR}$-Szilagyi was lower than $\overline{GR}$-Hydrus by 3.41 cm/year for all the AWDN sites or by 1.84 cm/year if the negative $\overline{GR}$ values were removed. Similar reasons for the discrepancy between $\overline{ET_a}$-Hydrus and $\overline{ET_a}$-MODIS could be attributed to the differences between $\overline{GR}$-Szilagyi and $\overline{GR}$-Hydrus. Overall, Figs. 7 and 8 show strong similarity of GR and ET_a estimates between model simulations and remotely sensed data.

3.4.2. Comparisons with tracer-based approaches

Allison et al. (1994) and De Vries and Simmers (2002) suggested that tracer-based approaches provided the most reliable GR

estimates; however, those approaches are generally expensive, which limits their applications to estimate *GR*. Several tracer-based studies were carried out in Nebraska to estimate *GR*, most notably in the Nebraska Sandhills. Szilagyi et al. (2011) compiled chloride data from 31 monitoring groundwater wells within the Nebraska Sandhills and applied the chloride mass balance method to quantify *GR* at those locations. Five sites, each within a radius of 20 km from an AWDN station, were identified from Szilagyi et al. (2011) and are shown in Fig. 1. The respective values of *GR* from Szilagyi et al. (2011) and the corresponding model simulations were 7.8 and 11.26 cm/year at Arthur, 10.3 and 7.04 cm/year at Barta, 0.9 and 2.17 cm/year at Cedar Point, 6.2 and 8.29 cm/year at Gothenburg, and 10.3 and 3.77 cm/year at Halsey. In addition, Adane and Gates (2015) applied both chloride and sulfate mass balance methods to estimate *GR* at an experimental site near Halsey, Nebraska, which was about 19 km from the AWDN station at Halsey. Under grass-covered conditions, Adane and Gates (2015) found *GR* to be 2.7 cm/year from the chloride mass method and 6.9 cm/year from the sulfate mass balance method. By comparison, $\overline{GR}$ at Halsey was 3.77 cm/year from the model simulations. Although the study sites of the above mentioned studies were not exactly at the locations of the AWDN sites, the *GR* estimates from the model simulations and tracer-based approaches were largely comparable in the Nebraska Sandhills. The findings reported here were consistent with the findings of Min et al. (2015), who also showed that *GR* estimated from model simulations was similar to the one obtained from the chloride mass balance method in an irrigated agricultural field.

3.4.3. Comparisons with regional water balance methods

Chen and Chen (2004) calibrated a regional groundwater flow model to observed groundwater levels in the eastern Nebraska Sandhills. Based on the model simulations, the authors found that about 13% of annual *P* went to recharge the underlying aquifer during the period between 1979 and 1990. Based on multidecadal *P* and streamflow data, Wang et al. (2009b) quantified water balance components in the catchments of the eastern Nebraska Sandhills with negligible anthropogenic disturbances and found that the ratio of $\overline{GR}/\overline{P}$ varied between 8% and 18% for those catchments. By comparison, the simulation results for the AWDN sites in the general area largely fell within the range of $\overline{GR}/\overline{P}$ from regional water balance analyses (e.g., 13.41%, 23.13%, 7.06%, and 9.50% at the sites of Barta, Elgin, Halsey, and Newport, respectively). In summary, based on the results from various approaches, the *GR* values from the model simulations were generally comparable in the study area, attesting to the feasibility of using large-scale soil moisture monitoring networks and inverse modeling for estimating spatial distributions of *GR*.

3.5. Soil and climatic controls on GR

Due to the highly nonlinear subsurface processes and their interactions with land surface processes, *GR* may vary substantially over space and time, depending on local conditions (e.g., soil, climate, and vegetation). It is thus important to understand the impacts of different controls on recharge processes. Given that the AWDN sites are covered by natural grasses, the modeling results were used to investigate soil and climatic controls on the spatiotemporal variability in *GR* across the study area.

Fig. 9 shows the relationships of $\overline{GR}$ and $\overline{GR}/\overline{P}$ with $\overline{P}$ and $\overline{ET_p}$ for all the AWDN sites. In general, $\overline{GR}$ showed similar patterns with $\overline{P}$ and $\overline{ET_p}$ to the ones of $\overline{GR}/\overline{P}$. On mean annual time scales, a positive correlation existed between $\overline{GR}/\overline{P}$ and $\overline{P}$; however, the correlation between $\overline{GR}/\overline{P}$ and $\overline{ET_p}$ was less clear. With increasing $\overline{P}$, $\overline{GR}/\overline{P}$ disproportionately increased, indicating that certain *P* thresholds

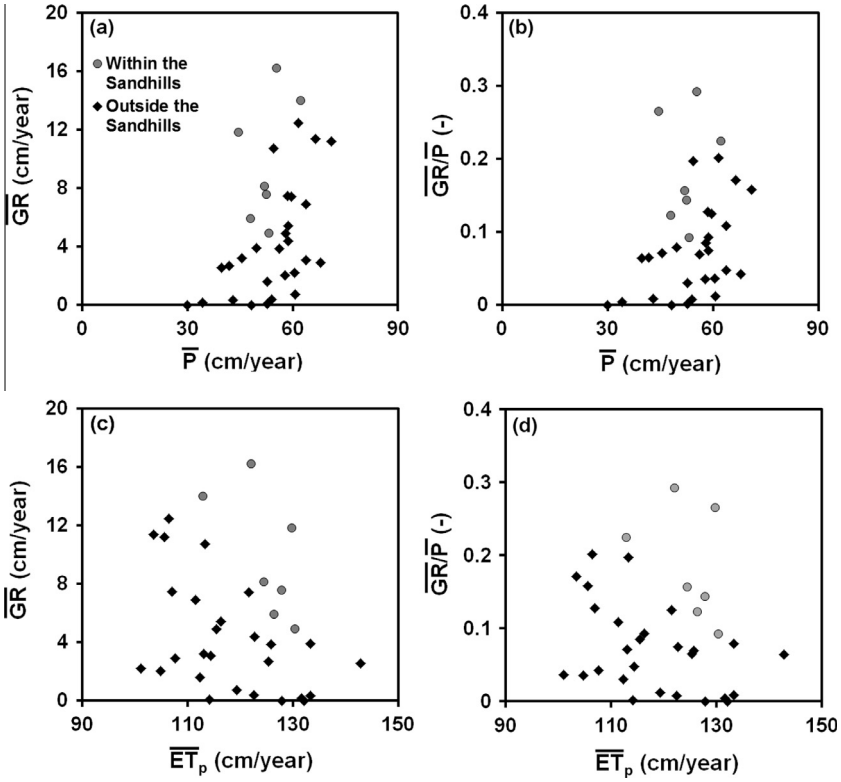

Fig. 9. Relationships of mean annual groundwater recharge ($\overline{GR}$) and recharge ratio ($\overline{GR}/\overline{P}$) with mean annual precipitation ($\overline{P}$) and potential evapotranspiration ($\overline{ET_p}$) at all AWDN sites.

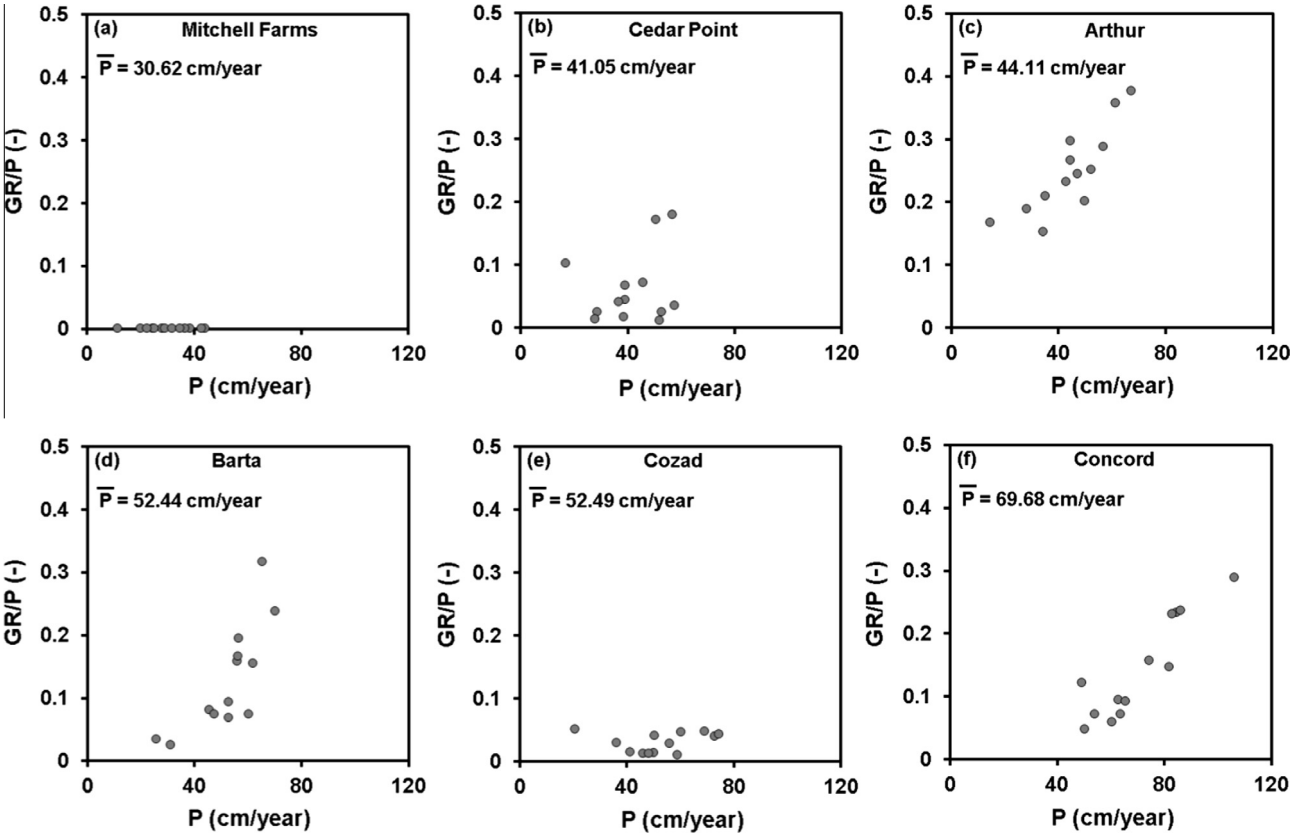

Fig. 10. Examples of the relationships between annual groundwater recharge ratio (GR/P) with annual precipitation (P) at individual AWDN sites.

were needed to meet the atmospheric demands for evapotranspiration before initiating recharge processes. Several reasons could be attributed to the weak correlation between $\overline{GR}/\overline{P}$ and $\overline{P}$. First, in addition to the total amount of P, other rainfall characteristics may also influence GR, such as rainfall intensity and duration (Small, 2005). Secondly, as shown in Figs. 4–6, soil properties played an important role in controlling soil moisture levels and thus relevant hydrological processes. Due to the soil textural differences in the study area (Istanbulluoglu et al., 2012), the extent of the Nebraska Sandhills was used to identify the AWDN sites with coarser-textured soils. It can be seen from Fig. 9 that under similar conditions of $\overline{P}$ and $\overline{ET_p}$, $\overline{GR}/\overline{P}$ were considerably larger for the AWDN sites within the Nebraska Sandhills. Fig. 9 reflects the significant control of soil texture on GR in the study area, which coincided with previous modeling and field studies (Keese et al., 2005; Wang et al., 2009b). Moreover, it demonstrates the capability of using inverse modeling approaches to capture the impacts of soil properties on subsurface hydrological processes.

For practical purposes, it is of importance to understand the relationship between P and GR (or GR/P) on annual time scales (Lu et al., 2011; Min et al., 2015; Turkeltaub et al., 2015). Examples of the relationships between annual P and GR/P are presented in Fig. 10 for the AWDN sites with contrasting climatic and soil conditions. Note that no lag time between P and GR was considered here, while delays can be expected for the deep drainage (i.e., below the root zones) to reach groundwater tables in the Nebraska Sandhills (Rossman et al., 2014). The relationships between annual P and GR/P differed significantly across the sites. Several observations can be made from Fig. 10. First, at Mitchell Farms, the insufficient inputs of P led to almost no response of GR/P to the variations in annual P. Secondly, with increasing P, the response of GR/P to variations in annual P gradually became stronger, depending on soil properties. In particular, compared to the sites outside the Nebraska Sandhills (e.g., Cedar Point and Cozad), the positive correlations between P and GR/P were much stronger at Arthur and Barta, regardless of $\overline{P}$ levels. This was consistent with the modeling results of Turkeltaub et al. (2015), who showed a strong positive correlation between P and GR in a semiarid sand dune area. With further increases in annual P (e.g., at Concord), a positive correlation between P and GR/P also emerged. Under similar levels of water inputs (e.g., P plus irrigation), Min et al. (2015) obtained a positive correlation between P and GR/P. It should be also noted that the characteristics of climatic conditions (e.g., climatic seasonality, and the frequency and intensity of storms) could also affect the ratio of GR/P (Small, 2005). Therefore, the different relationships between P and GR/P shown in Fig. 10 highlight the importance of scrutinizing those relationships at individual sites before application.

4. Conclusions

The feasibility of using inverse vadose zone modeling for estimating spatial distributions of groundwater recharge (GR) from large-scale soil moisture monitoring networks (>10^4 km^2) was demonstrated in this study. Long-term soil moisture data at 34 sites from the Automated Weather Data Network (AWDN) within Nebraska, USA were used to calibrate the Hydrus-1D model. With the help of the data in public domain and literature values for parameterization of the Hydrus-1D model, simulated soil moisture generally well matched the observed data under different soil and climatic conditions.

The mean annual GR estimated from the calibrated models varied over three orders of magnitude across the study area. To test the model results, estimates of GR and actual evapotranspiration

(ET_a) from the calibrated models were compared to the data obtained from other techniques from the study area, including remote sensing, tracer-based approaches, and regional water balance. Overall, the simulation results were comparable to *GR* and ET_a estimates from those techniques, attesting to the feasibility of using inverse modeling and large-scale soil moisture monitoring networks for estimating spatial distributions of *GR*.

The impacts of soil and climatic conditions on *GR* were assessed using the simulation results. The data showed that on mean annual time scales, both soil and precipitation (*P*) had significant impacts on *GR* in the study area with sandy soils generating higher *GR* under similar climatic conditions. On annual time scales, various relationships between *GR* and *P* emerged at the AWDN sites, depending on local soil and climatic conditions. In general, positive correlations between *GR* and *P* existed for the AWDN sites with coarser-textured soils or under wetter climatic conditions. Given the growing global network for soil moisture monitoring (Crow et al., 2012; Ochsner et al., 2013), data warehouses (Dorigo et al., 2011), and global datasets of soil texture (Shangguan et al., 2014), the proposed framework could be used to generate additional water balance flux datasets at various locations. Finally, it needs to note that this study only briefly discussed management implications of this work. A full assessment of aquifer sustainability should include inputs from a multitude of stakeholder groups in order to design pragmatic management strategies of this complex resource. In particular, large uncertainties associated with *GR* estimates as demonstrated in this study need to be taken into account when making water management decisions. Future studies are also needed to investigate the required density of soil moisture monitoring networks for estimating *GR* at catchment and regional scales using inverse modeling approaches.

Acknowledgments

The authors would like to thank the High Plains Regional Climate Center at the University of Nebraska for providing soil moisture and hydrometeorological data, and C. Finkenbiner at UNL for providing soil textural information. T.E. Franz, T.J. Wang, and V.A. Zlotnik acknowledge the support from the Daugherty Water for Food Institute at the University of Nebraska. Funding support was partially provided by the National Science Foundation's Integrated Graduate Education and Research Traineeship (IGERT) Program (Grant DGE-0903469) to V.A. Zlotnik. The authors would also like to dedicate this paper to Prof. Xunhong Chen in memory of his contributions to the field of hydrology.

Appendix A. Supplementary material

Supplementary data associated with this article can be found, in the online version, at http://dx.doi.org/10.1016/j.jhydrol.2015.12.019.

References

Abu-Awwad, A.M., 1997. Water infiltration and redistribution within soils affected by a surface crust. J. Arid Environ. 37 (2), 231–242. http://dx.doi.org/10.1006/jare.1997.0280.

Adane, Z.A., Gates, J.B., 2015. Determining the impacts of experimental forest plantation on groundwater recharge in the Nebraska Sand Hills (USA) using chloride and sulfate. Hydrogeol. J. 23 (1), 81–94. http://dx.doi.org/10.1007/s10040-014-1181-6.

Al-Kaisi, M.M., Elmore, R.W., Guzman, J.G., et al., 2013. Drought impact on crop production and the soil environment: 2012 experiences from Iowa. J. Soil Water Conserv. 68 (1), 19A–24A. http://dx.doi.org/10.2489/jswc.68.1.19A.

Allen, R.G., Pereira, L.S., Raes, D., Smith, M., 1998. Crop evapotranspiration: guidelines for computing crop water requirements. Irrig. Drain. Pap. 56, U. N. Food and Agric. Organ., Rome.

Allen, R.G., Pereira, L.S., Howell, T.A., Jensen, M.E., 2011. Evapotranspiration information reporting: I. Factors governing measurement accuracy. Agric. Water Manage. 98, 899–920. http://dx.doi.org/10.1016/j.agwat.2010.12.015.

Allison, G.B., Gee, G.W., Tyler, S.W., 1994. Vadose-zone techniques for estimating groundwater recharge in arid and semiarid regions. Soil Sci. Soc. Am. J. 58 (1), 6–14. http://dx.doi.org/10.2136/sssaj1994.03615995005800010002x.

Andreasen, M., Andreasen, L.A., Jensen, K.H., Sonnenborg, T.O., Bircher, S., 2013. Estimation of regional groundwater recharge using data from a distributed soil moisture network. Vadose Zone J. 12 (3). http://dx.doi.org/10.2136/vzj2013.01.0035.

Assefa, K.A., Woodbury, A.D., 2013. Transient, spatially varied groundwater recharge modeling. Water Resour. Res. 49, 4593–4606. http://dx.doi.org/10.1002/wrcr.20332.

Becker, M.W., 2006. Potential for satellite remote sensing of ground water. Groundwater 44 (2), 306–318. http://dx.doi.org/10.1111/j.1745-6584.2005.00123.x.

Böhlke, J.K., 2002. Groundwater recharge and agricultural contamination. Hydrogeol. J. 10 (1), 153–179. http://dx.doi.org/10.1007/s10040-001-0183-3.

Brunner, P., Doherty, J., Simmons, C.T., 2012. Uncertainty assessment and implications for data acquisition in support of integrated hydrologic models. Water Resour. Res. 48 (7), W07513. http://dx.doi.org/10.1029/2011WR011342.

Carrera-Hernández, J.J., Smerdon, B.D., Mendoza, C.A., 2012. Estimating groundwater recharge through unsaturated flow modelling: sensitivity to boundary conditions and vertical discretization. J. Hydrol. 452, 90–101. http://dx.doi.org/10.1016/j.jhydrol.2012.05.039.

Carsel, R.F., Parrish, R.S., 1988. Developing joint probability distributions of soil water retention characteristics. Water Resour. Res. 24, 755–769. http://dx.doi.org/10.1029/WR024i005p00755.

Chen, X., Chen, X., 2004. Simulating the effects of reduced precipitation on groundwater and streamflow in the Nebraska Sand Hills. J. Am. Water Resour. Assoc. 40, 419–430. http://dx.doi.org/10.1111/j.1752-1688.2004.tb01040.x.

Crow, W.T., Berg, A.A., Cosh, M.H., Loew, A., Mohanty, B.P., Panciera, R., Rosnay, P., Ryu, D., Walker, J.P., 2012. Upscaling sparse ground-based soil moisture observations for the validation of coarse-resolution satellite soil moisture products. Rev. Geophys. 50 (2), RG2002. http://dx.doi.org/10.1029/2011RG000372.

De Vries, J.J., Simmers, I., 2002. Groundwater recharge: an overview of processes and challenges. Hydrogeol. J. 10 (1), 5–17. http://dx.doi.org/10.1007/s10040-001-0171-7.

Dorigo, W.A., Wagner, W., Hohensinn, R., Hahn, S., Paulik, C., Xaver, A., Gruber, A., Drusch, M., Mecklenburg, S., van Oevelen, P., Robock, A., Jackson, T., 2011. The international soil moisture network: a data hosting facility for global in situ soil moisture measurements. Hydrol. Earth Syst. Sci. 15 (5), 1675–1698.

Faust, A.E., Ferré, T.P.A., Schaap, M.G., Hinnell, A.C., 2006. Can basin-scale recharge be estimated reasonably with water-balance models? Vadose Zone J. 5, 850–855. http://dx.doi.org/10.2136/vzj2005.0109.

Feddes, R.A., Kowalik, P.J., Neuman, S.P., 1978. Simulation of Field Water Use and Crop Yield. John Wiley and Sons, New York, NY.

Gleeson, T., Wada, Y., Bierkens, M.F., van Beek, L.P., 2012. Water balance of global aquifers revealed by groundwater footprint. Nature 488 (7410), 197–200. http://dx.doi.org/10.1038/nature11295.

Guber, A.K., Gish, T.J., Pachepsky, Y.A., van Genuchten, M.T., Daughtry, C.S.T., Nicholson, T.J., Cady, R.E., 2008. Temporal stability in soil water content patterns across agricultural fields. Catena 73, 125–133. http://dx.doi.org/10.1016/j.catena.2007.09.010.

Hopmans, J.W., Simunek, J., 1999. Review of inverse estimation of soil hydraulic properties. In: van Genuchten, M.Th., Leij, F.J., Wu, L. (Eds.), Proceedings of the International Workshop Characterization and Measurement of Hydraulic Properties of Unsaturated Porous Media. University of California, Riverside, pp. 643–659.

Hubbard, K.G., You, J., Sridhar, V., Hunt, E., Korner, S., Roebke, G., 2009. Near-surface soil–water monitoring for water resources in management on a wide-area basis in the Great Plains. Great Plains Res. 19, 45–54.

Istanbulluoglu, E., Wang, T.J., Wright, O.M., Lenters, J.D., 2012. Interpretation of hydrologic trends from a water balance perspective: the role of groundwater storage in the Budyko hypothesis. Water Resour. Res. 48 (3), W00H16. http://dx.doi.org/10.1029/2010WR010100.

Jackson, R.B., Canadell, J., Ehleringer, J.R., Mooney, H.A., Sala, O.E., Schulze, E.D., 1996. A global analysis of root distributions for terrestrial biomes. Oecologia 108, 389–411. http://dx.doi.org/10.1007/BF00333714.

Jiménez-Martínez, J., Skaggs, T.H., Van Genuchten, M.T., Candela, L., 2009. A root zone modelling approach to estimating groundwater recharge from irrigated areas. J. Hydrol. 367 (1), 138–149. http://dx.doi.org/10.1016/j.jhydrol.2009.01.002.

Kalma, J.D., McVicar, T.R., McCabe, M.F., 2008. Estimating land surface evaporation: a review of methods using remotely sensed surface temperature data. Surveys Geophys. 29, 421–469. http://dx.doi.org/10.1007/s10712-008-9037-z.

Keese, K.E., Scanlon, B.R., Reedy, R.C., 2005. Assessing controls on diffuse groundwater recharge using unsaturated flow modeling. Water Resour. Res. 41, W06010. http://dx.doi.org/10.1029/2004WR003841.

Kerr, Y.H., 2007. Soil moisture from space. Where are we? Hydrogeol. J. 15, 117–120. http://dx.doi.org/10.1007/s10040-006-0095-3.

Korus, J.T., Howard, L.M., Young, A.R., et al., 2013. The Groundwater Atlas of Nebraska, third ed. Conservation and Survey Division, School of Natural Resources, University of Nebraska, pp. 1–64.

Loope, D., Swinehart, J., 2000. Thinking like a dune field: geologic history in the Nebraska Sand Hills. Great Plains Res. 10, 5–35.

Lu, X., Jin, M., van Genuchten, M.T., Wang, B., 2011. Groundwater recharge at five representative sites in the Hebei Plain, China. Groundwater 49 (2), 286–294. http://dx.doi.org/10.1111/j.1745-6584.2009.00667.x.

Mahmood, R., Littell, A., Hubbard, K.G., You, J., 2012. Observed data-based assessment of relationships among soil moisture at various depths, precipitation, and temperature. Appl. Geogr. 34, 255–264.

Martinez-Fernandez, J., Ceballos, A., 2003. Temporal stability of soil moisture in a large-field experiment in Spain. Soil Sci. Soc. Am. J. 67, 1647–1656. http://dx.doi.org/10.2136/sssaj2003.1647.

Mason, J.A., 2001. Transport direction of Peoria Loess in Nebraska and implications for loess sources on the central Great Plains. Quaternary Res. 56, 79–86. http://dx.doi.org/10.1006/qres.2001.2250.

Maxwell, R.M., Kollet, S.J., 2008. Interdependence of groundwater dynamics and land-energy feedbacks under climate change. Nat. Geosci. 1 (10), 665–669. http://dx.doi.org/10.1038/ngeo315.

Miao, X., Mason, J.A., Swinehart, J.B., Loope, D.B., Hanson, P.R., Goble, R.J., Liu, X., 2007. A 10,000 year record of dune activity, dust storms, and severe drought in the central Great Plains. Geology 35, 119–122. http://dx.doi.org/10.1130/G23133A.1.

Min, L., Shen, Y., Pei, H., 2015. Estimating groundwater recharge using deep vadose zone data under typical irrigated cropland in the piedmont region of the North China Plain. J. Hydrol. 527, 305–315. http://dx.doi.org/10.1016/j.jhydrol.2015.04.064.

Mu, Q., Heinsch, F.A., Zhao, M., Running, S.W., 2007. Development of a global evapotranspiration algorithm based on MODIS and global meteorology data. Remote Sens. Environ. 111, 519–536. http://dx.doi.org/10.1016/j.rse.2007.04.015.

Mu, Q., Zhao, M., Running, S.W., 2011. Improvements to a MODIS global terrestrial evapotranspiration algorithm. Remote Sens. Environ. 115, 1781–1800. http://dx.doi.org/10.1016/j.rse.2011.02.019.

Mualem, Y., 1976. A new model for predicting the hydraulic conductivity of unsaturated porous media. Water Resour. Res. 12, 513–522. http://dx.doi.org/10.1029/WR012i003p00513.

Myneni, R.B., Hoffman, S., Knyazikhin, Y., Privette, J.L., Glassy, J., Tian, Y., Wang, Y., Song, X., Zhang, Y., Smith, Y., Lotsch, A., Friedl, M., Morisette, J.T., Votava, P., Nemani, R.R., Running, S.W., 2002. Global products of vegetation leaf area and fraction absorbed PAR from year one of MODIS data. Remote Sens. Environ. 83, 214–231. http://dx.doi.org/10.1016/S0034-4257(02)00074-3.

Nash, J., Sutcliffe, J.V., 1970. River flow forecasting through conceptual models part I – a discussion of principles. J. Hydrol. 10, 282–290. http://dx.doi.org/10.1016/0022-1694(70)90255-6.

National Research Council, 2004. Groundwater Fluxes Across Interfaces. Natl. Acad. Press, Washington, D.C.

Nolan, B.T., Healy, R.W., Taber, P.E., Perkins, K., Hitt, K.J., Wolock, D.M., 2007. Factors influencing ground-water recharge in the eastern United States. J. Hydrol. 332, 187–205. http://dx.doi.org/10.1016/j.jhydrol.2006.06.029.

Ochsner, T.E., Cosh, M.H., Cuenca, R.H., Dorigo, W.A., Draper, C.S., Hagimoto, Y., Kerr, Y.H., Larson, K.M., Njoku, E.G., Small, E.E., Zreda, M., 2013. State of the art in large-scale soil moisture monitoring. Soil Sci. Soc. Am. J. 77 (6), 1888–1919. http://dx.doi.org/10.2136/sssaj2013.03.0093.

Ries, F., Lange, J., Schmidt, S., Puhlmann, H., Sauter, M., 2015. Recharge estimation and soil moisture dynamics in a Mediterranean, semi-arid karst region. Hydrol. Earth Syst. Sci. 19 (3), 1439–1456. http://dx.doi.org/10.5194/hess-19-1439-2015.

Rossman, N.R., Zlotnik, V.A., Rowe, C.M., Szilagyi, J., 2014. Vadose zone lag time and potential 21st century climate change effects on spatially distributed groundwater recharge in the semi-arid Nebraska Sand Hills. J. Hydrol. 519, 656–669. http://dx.doi.org/10.1016/j.jhydrol.2014.07.057.

Scanlon, B.R., Faunt, C.C., Longuevergne, L., Reedy, R.C., Alley, W.M., McGuire, V.L., McMahon, P.B., 2012. Groundwater depletion and sustainability of irrigation in the US High Plains and Central Valley. Proc. Natl. Acad. Sci. 109 (24), 9320–9325. http://dx.doi.org/10.1073/pnas.1200311109.

Scanlon, B.R., Healy, R.W., Cook, P.G., 2002. Choosing appropriate techniques for quantifying groundwater recharge. Hydrogeol. J. 10, 18–39. http://dx.doi.org/10.1007/s10040-001-0176-2.

Scanlon, B.R., Keese, K.E., Flint, A.L., Flint, L.E., Gaye, C.B., Edmunds, W.M., Simmers, I., 2006. Global synthesis of groundwater recharge in semiarid and arid regions. Hydrol. Process. 20, 3335–3370. http://dx.doi.org/10.1002/hyp.6335.

Schaap, M.G., Leij, F.J., van Genuchten, M.T., 2001. Rosetta: a computer program for estimating soil hydraulic parameters with hierarchical pedotransfer functions. J. Hydrol. 251, 163–176. http://dx.doi.org/10.1016/S0022-1694(01)00466-8.

Shangguan, W., Dai, Y., Duan, Q., Liu, B., Yuan, H., 2014. A global soil data set for earth system modeling. J. Adv. Model. Earth Syst. 6, 249–263. http://dx.doi.org/10.1002/2013MS000293.

Small, E.E., 2005. Climatic controls on diffuse groundwater recharge in semiarid environments of the southwestern United States. Water Resour. Res. 41, W04012. http://dx.doi.org/10.1029/2004WR003193.

Šimunek, J., Šejna, M., Saito, H., Sakai, M., van Genuchten, M.T., 2013. The HYDRUS-1D Software Package for Simulating the One-Dimensional Movement of Water, Heat, and Multiple Solutes in Variably-Saturated Media, Version 4.17. Department of Environmental Sciences, University of California Riverside, Riverside, California, USA, 307 pp.

Soylu, M.E., Istanbulluoglu, E., Lenters, J.D., Wang, T.J., 2011. Quantifying the impact of groundwater depth on evapotranspiration in a semi-arid grassland region. Hydrol. Earth Syst. Sci. 15 (3), 787–806. http://dx.doi.org/10.5194/hess-15-787-2011.

Szilagyi, J., Harvey, F.E., Ayers, J.F., 2003. Regional estimation of base recharge to ground water using water balance and a base-flow index. Groundwater 41, 504–513. http://dx.doi.org/10.1111/j.1745-6584.2003.tb02384.x.

Szilagyi, J., Zlotnik, V.A., Gates, J.B., Jozsa, J., 2011. Mapping mean annual groundwater recharge in the Nebraska Sand Hills, USA. Hydrogeol. J. 19 (8), 1503–1513. http://dx.doi.org/10.1007/s10040-011-0769-3.

Szilagyi, J., Jozsa, J., 2013. MODIS-aided statewide net groundwater-recharge estimation in Nebraska. Groundwater 51 (5), 735–744. http://dx.doi.org/10.1111/j.1745-6584.2012.01019.x.

Trambauer, P., Dutra, E., Maskey, S., Werner, M., Pappenberger, F., Van Beek, L.P.H., Uhlenbrook, S., 2014. Comparison of different evaporation estimates over the African continent. Hydrol. Earth Syst. Sci. 18, 193–212. http://dx.doi.org/10.5194/hess-18-193-2014.

Turkeltaub, T., Kurtzman, D., Bel, G., Dahan, O., 2015. Examination of groundwater recharge with a calibrated/validated flow model of the deep vadose zone. J. Hydrol. 522, 618–627. http://dx.doi.org/10.1016/j.jhydrol.2015.01.026.

van Genuchten, M.T., 1980. A closed-form equation for predicting the hydraulic conductivity of unsaturated soils. Soil Sci. Soc. Am. J. 44, 892–898. http://dx.doi.org/10.2136/sssaj1980.03615995004400050002x.

Vrugt, J.A., Stauffer, P.H., Wöhling, Th., Robinson, B.A., Vesselinov, V.V., 2008. Inverse modeling of subsurface flow and transport properties: a review with new developments. Vadose Zone J. 7, 843–864. http://dx.doi.org/10.2136/vzj2007.0078.

Wang, T.J., Zlotnik, V.A., 2012. A complementary relationship between actual and potential evapotranspiration and soil effects. J. Hydrol. 456, 146–150. http://dx.doi.org/10.1016/j.jhydrol.2012.03.034.

Wang, T.J., Franz, T.E., Zlotnik, V.A., 2015a. Controls of soil hydraulic characteristics on modeling groundwater recharge under different climatic conditions. J. Hydrol. 521, 470–481. http://dx.doi.org/10.1016/j.jhydrol.2014.12.040.

Wang, T.J., Franz, T.E., Zlotnik, V.A., You, J., Shulski, M.D., 2015c. Investigating soil controls on soil moisture spatial variability: numerical simulations and field observations. J. Hydrol. 524, 576–586. http://dx.doi.org/10.1016/j.jhydrol.2015.03.019.

Wang, T.J., Istanbulluoglu, E., Lenters, J., Scott, D., 2009b. On the role of groundwater and soil texture in the regional water balance. An investigation of the Nebraska Sand Hills, USA. Water Resour. Res. 45, W10413. http://dx.doi.org/10.1029/2009WR007733.

Wang, T.J., Istanbulluoglu, E., Wedin, D., Hanson, P., 2015d. Impacts of devegetation on the temporal evolution of soil saturated hydraulic conductivity in a vegetated sand dune area. Environ. Earth Sci. 73 (11), 7651–7660. http://dx.doi.org/10.1007/s12665-014-3936-8.

Wang, T.J., Wedin, D.A., Franz, T.E., Hiller, J., 2015b. Effect of vegetation on the temporal stability of soil moisture in grass-stabilized semi-arid sand dunes. J. Hydrol. 521, 447–459. http://dx.doi.org/10.1016/j.jhydrol.2014.12.037.

Wang, T.J., Zlotnik, V.A., Šimunek, J., Schaap, M.G., 2009a. Using pedotransfer functions in vadose zone models for estimating groundwater recharge in semiarid regions. Water Resour. Res. 45, W04412. http://dx.doi.org/10.1029/2008WR006903.

Wang, T.J., Zlotnik, V.A., Wedin, D., Wally, K.D., 2008. Spatial trends in saturated hydraulic conductivity of vegetated dunes in the Nebraska Sand Hills: effects of depth and topography. J. Hydrol. 349, 88–97. http://dx.doi.org/10.1016/j.jhydrol.2007.10.027.

Wen, F., Chen, X., 2006. Evaluation of the impact of groundwater irrigation on streamflow in Nebraska. J. Hydrol. 327 (3), 603–617. http://dx.doi.org/10.1016/j.jhydrol.2005.12.016.

Wösten, J.H.M., Pachepsky, Y.A., Rawls, W.J., 2001. Pedotransfer functions: bridging the gap between available basic soil data and missing soil hydraulic characteristics. J. Hydrol. 251, 123–150. http://dx.doi.org/10.1016/S0022-1694(01)00464-4.

Zlotnik, V.A., Wang, T., Nieber, J.L., Simunek, J.A., 2007. Verification of numerical solutions of the Richards equation using a traveling wave solution. Adv. Water Resour. 30, 1973–1980. http://dx.doi.org/10.1016/j.advwatres.2007.03.008.